CONTRIBUTION OF NON-LINEAR STRUCTURE TO THE KINETIC SUNYAEV-ZELDOVICH POWER SPECTRUM

by

Yang Liu

M.Sc., Shandong University & University Of Chinese Academy Of Sciences, 2010

B.Sc., Shandong University, 2007

A Thesis submitted in partial fulfillment
of the requirements for the degree of

MASTER OF SCIENCE

in the
Department of Physics
Faculty of Science

SIMON FRASER UNIVERSITY
Spring 2013

APPROVAL

Name: Yang Liu

Degree: MASTER OF SCIENCE

Title of Thesis: CONTRIBUTION OF NON-LINEAR STRUCTURE TO THE KINETIC SUNYAEV-ZELDOVICH POWER SPECTRUM

Examining Committee:

Dr. J. Steven Dodge, Chair
Associate Professor

Dr. Levon Pogosian, Senior Supervisor
Associate Professor

Dr. Andrei Frolov, Supervisor
Associate Professor

Dr. Howard Trottier, Supervisor
Professor

Dr. Dugan O'Neil, Internal Examiner
Associate Professor

Date Approved: February 6, 2013

Partial Copyright Licence

Abstract

In the last two decades, a satisfactory standard cosmological model has been established. On the other side, a wealth of new precise data from various astronomical observations is becoming available, leading to increased interest in details of the CMB foreground physics. In this thesis we investigate a very promising foreground effect, the kinetic Sunyaev-Zeldovich (kSZ) effect, and calculate its contribution to the CMB power spectrum. The kSZ effect is due to the interaction of CMB photons with a moving structure between the observer and the surface of last scattering, such as a cluster of galaxies, that contains ionized gas and moves with a certain peculiar velocity. The strength of the effect is determined by both the non-linear density distribution of matter inside clusters and the peculiar velocity which is governed by the linearly perturbed matter density around them. We analyze the relative importance of the the linear and non-linear contributions to the kSZ considering only gravitational interactions. We find that the non-linear contribution significantly changes the power spectrum at very small scales, thus we believe including baryonic physics, which also governs the nonlinear evolution of the structures, is necessary. The effect of baryons is to redistribute matter toward the centres of halos, which can be dramatic when the baryon component is allowed to cool. We calculate this deviation as well as its impact on the kSZ CMB power spectrum.

Acknowledgments

Beyond all of the acknowledgement, I would like to present my greatest thanks to my senior supervisor, Dr. Levon Pogosian. I really appreciate for his supervision and supports. Dr.Levon can always express issues in a simplest manner and right to the point, but I believe what I learn most from him is the way and attitude in handling stuffs in daily life. Dr. Levon is one of the most nice person I have ever known.

I would also like to thank the other members of my examining committee, Dr. J. Steven Dodge, Dr. Andrei Frolov, Dr. Howard Trottier and Dr. Dugan O'Neil for their valuable comments. Also for their attending my examination with sparing time even at their inconvenience and busy hour.

The Department of Physics at Simon Fraser University (SFU) is such an encouraging and thoughtful place where College life and activities are also very much an important part of three year life at SFU. It is a wonderful place to meet many smart and eminent people in every different subject. It is a place to learn about the world. I would also like to sincerely thank all the members in our Cosmology Group at SFU, in particular, Dr. Aliriza, Jun-Qi, Yun, Hasmik, Starla, Shao-Jie, Aaron, Andrei and Levon. I will miss everyone of you.

Furthermore, I would like to thank my fantastic friends Sam, Sumter, Kai Geng, Gavin, Lucas, Chao Liu, Wen Huang, Jixin Liang, James Zhang, willy, Si-Meng, Peter, John, Rudi, April Sun et al.. I know they are less likely to read this thesis but they really deserve thanks.

I also want to express my thanks to Yin-Zhe Ma, who currently carries on his postdoc research at University of British Columbia in Canada, and Sheng Li, who is currently a PhD

student at University of Sussex in UK. Both two colleagues are the best friends of mine who can give suggestion and chat while I suffered from life or study. From Yin-Zhe I learned much on doing research and life, and from Sheng much helps in numerical programming. Also they helped me a lot in completing this work.

Last but not least, completing a MSc study is not possible without the unwavering support from my family and closest people. I would like to express my thanks to the encouraging supports and considerable understandings from my beloved girlfriend: Su-Qi Cheng. I also would like to thank my parents, Wei-Ying Wang and Jian-Guo Liu, as well as other family members, for their constant love and supports.

Contents

Chapter 1

Introduction

Cosmology studies the origin, evolution and destination of our Universe (or Multiverse) as well as the natural laws behind it, based on scientific observations and experiments.

By studying ancient calendars, science historians believe that the history of Cosmology is as long as the history of civilization. Time flies by. It has, once again, became one of the most quickly developing branches of Physics due to the launch of various observational projects. Those cosmological observations enabled human beings to enter the era of precision cosmology. More specifically, grouped by general approaches, there are six categories of observations:

- Traditional Telescope Observations
  Use not only visible light, but the spectrum ranging from radio to gamma-rays. However, ground-based observations are limited by atmospheric effects
- Redshift Surveys
  Scan and map the 3D distribution of matter by counting numbers of galaxies, such as 2dFGRS[1], SDSS [2]
- Cosmic Microwave Background (CMB) Experiments
  Measure the relics of a time when the universe was hot and dense and extract the abundant information encoded in it, such as COBE [3], WMAP [4], Planck [5]
- Cosmic Neutrinos Background
  Carries plenty of information but may be impossible to extract, could be a future

window

- Gravitational Waves
  Detection of the disturbance of the space - time
- Cosmic Ray Observation
  Detect the randomly distributed ultra high energy particles rather than electromagnetic waves, mostly relevant to astrophysical phenomena

The first two approaches are most important in exploring the evolution history of the universe, in which telescope observations and redshift surveys focus on local effects and can probe relatively late celestial physics, while CMB experiments measure global statistical features and can reach a much earlier stage of the evolution history of the universe. In fact, combining these two very different approaches by considering their junction is a motivation of our work.

Cosmic Neutrinos Background is a potential treasure that we are far away to from taking advantage of. The last two approaches, Gravitational Waves and Cosmic Rays, on the other hand, are of importance to theories of high energy physics, especially in Gravity quantization and string theory.

As a subject in physics, cosmology is based on experiments, However, rather than simple induction from experiments results, cosmology relies more on theoretical extrapolations not only because the energy scale is far higher than human's reaches but also because we can not re-create the universe and do the observation as in other areas of physics.

This is the reason why cosmology is often about "models", either proposing a new yet reasonable one or verifying it with the data from variety of experiments mentioned above. Our work belongs to the later, which is using the CMB power spectrum to constrain models of gravity.

Fortunately, the experiment's results are compatible with the high energy theories and their extrapolations, and we now have a standard model of cosmology except there are still three unknown components. These are inflation, dark matter and dark energy. We know their effect on the evolution of the universe but little about their physical character.

More specifically, the observations strongly support a spatially flat Universe which is accelerating at the present day, consisting of approximately 73% dark energy, 23% cold dark matter (CDM), 4% baryons as well as negligible radiation. To explain why the space is so flat and some other problems in Big Bang theory, scientists introduced Inflation, a special period of time when the Universe was expanding exponentially. Soon, an unexpected yet significant byproduct of inflation was found: it provides the Universe with the seeds for today's inhomogeneous large scale structure. During Inflation, tiny quantum fluctuations of space-time background were stretched out of horizon and became frozen. The simplest inflationary paradigm provides an adiabatic, Gaussian and nearly scale-invariant fluctuations which are consistent with the CMB observations.

When these fluctuations reenter the horizon at late times, curvature perturbations work as potential wells making CDM and baryons collapse, leaving two important signatures on the sky that we can observe today. One is the imprint on the CMB, where acoustic oscillation peaks are generated in the angular power spectrum. The other is the cosmic structure that we observe today, which would be amplified by gravitational instability to produce nonlinear structures, such as galaxies and clusters.

Now we have the Friedmann-Robertson-Walker (FRW) metric as space and time background; we have scale invariant primordial perturbations as initial conditions; we have particle components such as CDM, baryons, photons, neutrinos, which could have interactions governed by the four basic forces. Putting these together and using Conservation Equations, Einsteins Equations of General Relativity, one can get physical observables compatible with today's experiment's results which surely is a big triumph of the most fundamental physics theories as well as their extrapolations.

In this standard procedure, the key points connecting the observation results and the theoretical predictions are two spectrums. First, telescope observations and redshift surveys [6, 7, 8] are used to infer the matter power spectrum, P(k), which shows the distribution of the matter density fluctuations on different scales to a fairly high precision. Second, CMB experiments, such as the satellite observations (WMAP [9, 10, 11] and Planck [12]), ground-based telescopes (ACBAR [13], BICEP-II [14], QUIJOTE [15], PolarBear [16], QUIET [17]), balloon-borne experiments (EBEX [18] and Spider [19]), similarly, measure power spectrum,

C_l of the CMB temperature fluctuations, which shows temperature fluctuations on different angular scales. Various authors have developed codes, such as CMBFAST [20] and CAMB [21], to compute the linear part of the power spectrum widely used in testing models. These two power spectra were tightly correlated in the very early stage since the beginning of the Universe(beginning of the Big Bang usually refer to the end of the reheating after inflation). But after the decoupling of matter from radiation, they were considered to evolve independently in the simplest picture.

However, beyond this simplest picture there is plenty of interesting foreground physics, because after last scattering, the photons traveling across the Universe respond not only to the perturbations in the space-time metric but also to the charges (although the ratio of charge density to cross-section is generally very small). These corrections to photon's motion are extremely tiny, yet, we are in an era that the experiments mentioned above just had or are going to have the ability to distinguish this level of small variations. This makes the corresponding research very active and exciting.

The photons traveling through the universe from the last scattering surface can interact with all kinds of matter via the gravitational force:

- The Integrated Sachs-Wolfe Effect [22]
  Photons falling into a gravitational potential will gain energy. If the potential evolves with time, the energy lost climbing out of that potential well will be different from that gained before, leading to a net anisotropy. The gravitational potential ϕ is constant when matter dominates the energy budget. However, this in not true ($\dot{\phi} \neq 0$)both in the early("Early ISW Effect") and late("Late ISW Effect") times where radiation and dark energy make a large contribution respectively.
- The Rees-Sciama Effect [23]
  As photons pass through the time-changing potentials formed by non-linear structures due to the growth and movement of its bound, anisotropy occurs. This effect is typically very small. People use Rees-Sciama as well as the late ISW effect to explain the mystery "cold spot" in the WMAP.
- The Gravitational Lensing [24]

In addition to the energy gained and lost, the photon's path will also be altered by potentials. Non-linear matter object such as cluster of galaxies creates a potential well bending the lights from the source, as it travels towards the observer. Gravitational lensing can be used to reconstruct the mass distribution creating the potential well.

The photons traveling through the universe from the last scattering surface can interact with charges via electromagnetic force:

- The Reionization
  As first stars formed, they radiated energy, ionizing neutral hydrogen. The universe went back to being an ionized plasma again. Because baryons(plasma) and photons had decoupled since recombination, these two fluids can have a large relative velocity enhancing the power due to the Doppler scattering. The second order effect know as the Ostriker-Vishniac effect[25].

- The Sunyaev-Zel'dovich Effect
  Once structure formation is well underway, nonlinear structures, the hot gas in the intergalactic medium for instance, can achieve very high temperature and probably a huge Virial speed. These moving charges can increase the CMB photon's energy through inverse-Compton-scattering known as Sunyaev-Zel'dovich Effect[26, 27, 28].

All these "foreground"effects have plenty of interesting and unique features, moreover, they all have a common theme or they are all about one thing: "**How The Photons We Observed Are Affected By Matter Throughout The Whole History Of The Universe?"** They are the bridges connecting the CMB angular power spectrum and the matter power spectrum. Among them, Sunyaev-Zel'dovich Effect is most promising because it happens at relatively late time so that the effect is easier to detect, while the very early effects such as ISW or Rees-Sciama effect is sort of "blurred"since they are seen in combination with many other effects.

In this thesis we investigate the kinetic Sunyaev-Zeldovich (kSZ) effect. We will not focus on the physics details of this effect such as scattering, frequency character or observation techniques. We see it as a bridge connecting density anisotropy and CMB anisotropy. We calculate kSZ's contribution to the CMB power spectrum.

In Chapter 2, we briefly introduce the Cosmological Standard Model including some fundamental principles and the explanation of today's anisotropy in both matter and CMB photons. In Chapter 3, we come back to the kSZ effect, which arises if the scattering medium is moving relative to the Hubble flow, so that the fractional temperature change is proportional to the density-weighted-velocity. After calculating the power spectrum of kSZ, we find that kSZ is sensitive to the details of reionization. The strength of the effect is determined by both the non-linear density distribution of matter inside clusters and the peculiar velocity which is governed by the linearly perturbed matter density around them. We analyze the relative importance of the linear and non-linear contributions to the kSZ. We find that the non-linear velocity perturbations' contribution is small both in magnitude and scale. We then go beyond the linear perturbation theory, using non-linear density power spectrum $P_{\delta\delta}^{NL}$ to get kSZ power spectrum and found that the non-linear density modification have relatively larger impact. There are also suggestions that if some baryonic processes are considered, especially when the radial direction cooling and star formation are included, the kSZ power spectrum might be changed significantly. Thus we believe that including baryonic physics which also governs the nonlinear evolution of the structures is necessary. In Chapter 4, we first find that the thermal pressure of the baryons decreases the kSZ signal slightly, then we calculate the new matter power spectrum with baryonic cooling and star formation(CSF), form which we find that CSF can change the kSZ power spectrum significantly. Chapter 5 is conclusion and outlook, where we indicate that kSZ effect can be used to test gravity.

Chapter 2

Standard Cosmology

During the 1940's, based on the observed Hubble expansion, Gamow et.al. proposed that the Universe originated from a extremely hot and dense state[29]. At the same time, Bondi, Fred Hoyle and Gold, who believed the Universe is steady and everlasting, on the other hand, proposed the continuous creation model or the so called "steady-state Universe"[30]. In the steady-state scenario, to maintain a steady density in an expanding Universe, matter must be created but only at an extremely low rate required to be compatible with observations, and the advantages are that it does not have a series of big problems[31, 32, 33, 34, 35] encountered in Gamow's Big Bang scenario such as the causality problem, the horizon problem and the entropy problem. As a competitor, Fred Hoyle was on a radio show to advocate the Steady State Model, and referred to Gamow's expanding universe model as "the big bang idea". These opposite theories fought each other for decades until the discovery of the Cosmic Microwave Background in 1960s[36] provided experimental validation of the Big Bang idea. Still, the debate continued because of the above mentioned problems.

In the 1980s, the proposal of inflation[37, 38] dramatically changed this situation. Inflation elegantly solved all of the above mentioned severe problems in Big Bang scenario, and therefore, we now have a Cosmological Standard model [1]. Inflation also helps the BigBang idea by successfully predicting later confirmed adiabatic, Gaussian and nearly scale-invariant primordial fluctuations[39] which the question of where the structure comes from. In this

[1] Although the steady-state scenario lost the battle, the belief that the Universe is infinite to the past and to the future continues. There are bounce and cyclic Universe models being studied such as Steinhardt and Turok's oscillation theory[40, 41].

Chapter, we very briefly introduce the standard model of Cosmology.

2.1 Principles of Cosmology

The Cosmological Principle is an working assumption preferred by large scale observations. It is a foundation of modern cosmology which combined with Einstein equations determine the evolution of the space and time in our Universe[2].

Cosmological Principle, which is a strongly philosophical one, normally states that the properties of the Universe are the same when viewed by all observers separated by a sufficiently large scale. This statements indicates that not only the mean physical structures, but also the effects of physical laws in observable phenomena are the same at different parts of the Universe. It is therefore hard to say that the space-time we live in is unique. As a matter of fact, observations suggest that our universe is homogeneous and isotropic on cosmological scales. Within small scales of our observed universe, there exists a large amount of anisotropy, but this anisotropy is getting smaller when one looks at larger scales. Generally, the universe appears homogeneous and isotropic on scales larger than $100Mpc$ [3].

From this assumption, we have a metric which describes this homogeneous and isotropic universe named as Friedmann-Robertson-Walker (FRW) metric [42],[43],

$$ds^2 = -dt^2 + a^2(t)\left[\frac{dr^2}{1-kr^2} + r^2(d\theta^2 + \sin^2\theta d\phi^2)\right] \tag{2.1}$$

where the scale factor is denoted by a time dependent function $a(t)$. The universe under this metric expands as the factor scale is increasing, while the universe contracts as this factor decreasing. r, θ, ϕ are three components in polar coordinate system, which is labeled as comoving system; accordingly the spatial curvature of hyper-surface in this system takes

[2]There are also studies on the expansion of the space and time as a result of an anisotropic Universe such as John Barrow's work[44, 45].

[3]Since there is a difficulty in observing the patch of space with large redshift z and large scale, the present researches intend to investigate our observed universe beyond the cosmological principle. For example, some people claim that the acceleration of universe might be the apparent effect due to the odd distribution of energy or matter[46, 47, 48]. And CMB observation indicate that there might be dipole asymmetry(anisotropy) even when the particular velocity effect is deducted, and that in CMB there exists a huge "cold spot"[49] which could be interpreted as a large "void" with radius at least as large as $300Mpc$ around that direction in the sky[50].

value $k = 0, \pm 1$ which depends on the type of spatial property. If $k > 0$, the universe is finite and unbounded, and infinite and unbounded if $k \leq 0$.

In the FRW metric, time t is the proper time which could be regarded as the standard time scale for the evolution of the universe. We could also derive the following conclusions for our universe,

$$\begin{aligned} \dot{a} > 0 \quad &\Leftrightarrow \quad \text{Expanding Universe} \\ \dot{a} = 0 \quad &\Leftrightarrow \quad \text{Static Universe} \\ \dot{a} < 0 \quad &\Leftrightarrow \quad \text{Contracting Universe} \end{aligned}$$

Assuming that a light started traveling from a galaxy at $t = t_1$, and is received by an observer at $t = t_0$, using $ds^2 = 0$ we obtain,

$$\int_{t_1}^{t_0} \frac{dt}{a\,(t)} = \int_0^{r_1} \frac{dr}{\sqrt{1 - kr^2}} \tag{2.2}$$

After an elapsed of time $(t_1 + \Delta t_1)$, another light starts traveling again from this galaxy, the receiving time will become $(t_0 + \Delta t_0)$ at the place $r = 0$ where the observer stands, then we have

$$\int_{(t_1 + \Delta t_1)}^{t_0 + \Delta t_0} \frac{dt}{a\,(t)} = \int_0^{r_1} \frac{dr}{\sqrt{1 - kr^2}} \tag{2.3}$$

Connecting Eq. (2.2) and Eq. (2.3) we get

$$\frac{\Delta t_0}{\Delta t_1} = \frac{a(t_0)}{a(t_1)} \tag{2.4}$$

Therefore, the observed redshift can be written as

$$z \equiv \frac{\lambda_0 - \lambda_1}{\lambda_1} = \frac{\Delta t_0 - \Delta t_1}{\Delta t_1} = \frac{a(t_0)}{a(t_1)} - 1 \tag{2.5}$$

So far, we can conclude that,

$$\begin{aligned} z > 0 \text{ , Redshift} \quad &\Rightarrow \quad a(t_0) > a(t_1) \quad \Rightarrow \quad \text{Expansion} \\ z = 0 \text{ , Non-shift} \quad &\Rightarrow \quad a(t_0) = a(t_1) \quad \Rightarrow \quad \text{Stable} \\ z < 0 \text{ , Blueshift} \quad &\Rightarrow \quad a(t_0) < a(t_1) \quad \Rightarrow \quad \text{Contraction} \end{aligned}$$

Current observations show redshift, which means our universe is expanding.

The energy-momentum tensor indicates that the elements defined in the metric (2.1) are of symmetry,

$$T^{\mu}_{\nu} = \text{Diag}\left(-\rho(t), p(t), p(t), p(t)\right) . \tag{2.6}$$

where the meaning of $\rho\,, p$ will be stated below.

2.2 Dynamics of Expansion

Given the FRW metric, we can find the law for scale factor a = a(t) using the Einstein field equation,

$$G^{\mu}_{\nu} \equiv R^{\mu}_{\nu} - \frac{1}{2}\delta^{\mu}_{\nu}R = 8\pi G T^{\mu}_{\nu} \tag{2.7}$$

where G^{μ}_{ν} is the Einstein Tensor, and R^{μ}_{ν} the Ricci Tensor, while R is the Ricci Scalar, and T^{μ}_{ν} is the Momentum-Energy Tensor, and δ^{μ}_{ν} is the Kronecker symbol.
We now derive the Friedmann Equation beginning with deriving Ricci tensor and its scalar form,

$$R^{0}_{0} = \frac{3\ddot{a}}{a}\,, \tag{2.8}$$

$$R^{i}_{j} = \left(\frac{\ddot{a}}{a} + \frac{2\dot{a}^2}{a^2} + \frac{2k}{a^2}\right)\delta^{i}_{j}\,, \tag{2.9}$$

$$R = 6\left(\frac{\ddot{a}}{a} + \frac{\dot{a}^2}{a^2} + \frac{k}{a^2}\right)\,, \tag{2.10}$$

Besides, for the consistency with the symmetry of the FRW metric, it is demanded that the total momentum-energy tensor must be diagonal and isotopic, which means the spatial part of T^{μ}_{ν} must be identical. The simplest realization is taking the momentum-energy tensor of fluid which has the following form,

$$T^{\mu}_{\nu} = \text{Diag}\left(-\rho, p, p, p\right)\,, \tag{2.11}$$

where both the energy density ρ and pressure p are function of time t. Substituting Eqs. (2.8 2.11) into field equation (2.7) we can obtain the FRW equations:

$$H^2 \equiv \left(\frac{\dot{a}}{a}\right)^2 = \frac{8\pi G\rho}{3} - \frac{k}{a^2} \tag{2.12}$$

$$\dot{H} = -4\pi G(p+\rho) + \frac{k}{a^2}\,, \tag{2.13}$$

where $H = \frac{\dot{a}}{a}$ is the Hubble parameter with its present value $H_0 = 70.5 \pm 1.3 kms^{-1}Mpc^{-1}$. If we define the critical density ρ_c and dimensionless parameter Ω as

$$\rho_c \equiv \frac{3H^2}{8\pi G} \quad \Omega \equiv \frac{\rho}{\rho_c}, \tag{2.14}$$

then Eq. (2.12) can be rewritten as

$$\Omega(t) - 1 = \frac{K}{(aH)^2}, \tag{2.15}$$

According to this equation, the structure of the background space-time is determined by the matter distributed in it , that is:

$$\begin{aligned} \Omega > 1 \quad \text{Or} \quad \rho > \rho_c \quad &\rightarrow \ K = +1 \\ \Omega = 1 \quad \text{Or} \ \rho = \rho_c \quad &\rightarrow \ K = 0 \\ \Omega < 1 \quad \text{Or} \ \rho < \rho_c \quad &\rightarrow \ K = -1 \end{aligned}$$

The current observational data implies that our universe is almost flat, therefore $\Omega \simeq 1$, $K = 0$ [4].

From the energy conservation law, we can obtain the continuity equation,

$$\dot{\rho} + 3H(\rho + p) = 0 \ . \tag{2.16}$$

Since Eq. (2.16) can also be derived from combining both Eq. (2.12) and Eq. (2.13), only two among those three equations are independent.
Besides, from Eq. (2.12) and Eq. (2.13) we can have

$$\frac{\ddot{a}}{a} = -\frac{4\pi G}{3}(\rho + 3p) \tag{2.17}$$

Thus, now we've got a critical value $\rho + 3p$ which determines the sign of $\ddot{a}$. The fact that our observable universe is expanding with positive acceleration requires $\rho + 3p < 0$ today. Considering when $k = 0$, Eq. (2.12), Eq. (2.17) can also be expressed as,

$$\dot{H} = -4\pi G(\rho + p) \tag{2.18}$$

[4] This is a result of inflation in the early stage of our universe.

This equation suggests that if $p = -\rho$, the Hubble constant H and, therefore, the energy density remain constant as the Universe expands. The increase in the energy comes from the work done by the negative pressure,

$$d(\rho a^3) = -pd(a^3) \tag{2.19}$$

providing a way of solving the entropy problem[5] encountered in the Big Bang.

Provided that the equation of state has the form $p = p(\rho)$, we can determine the energy density as a function of the scale factor a. For example, if the energy density ρ of the universe is dominated by non-relativistic matter for which pressure p can be neglected, we can derive the following relation from Eq. (2.19)

$$\rho \propto a^{-3} \quad p \ll \rho; \tag{2.20}$$

while if it is dominated by relativistic particles, we obtain,

$$\rho \propto a^{-4} \quad p = \frac{\rho}{3}. \tag{2.21}$$

From the energy function above together with Eq. (2.12) we will obtain the scale factor $a(t)$. The particular form of function $a(t)$ determines different process of the evolution of our universe. And the final stage of the evolution could be determined by the initial conditions.

As a matter of fact, we could define the state equation as $p = w\rho$ in which w is a constant and includes two major components which are:

- Relativistic Particle: $w = 1/3$;
- Non-relativistic Matter: $w = 0$.

Under this circumstance, from continuity equation we can obtain

$$\rho \propto a^{-3(1+w)}. \tag{2.22}$$

and by substituting it into the Eq. (2.12), we will have

$$3\frac{\dot{a}^2}{a^2} = 8\pi G\rho_0 \left(\frac{a}{a_0}\right)^{-3(1+w)}. \tag{2.23}$$

[5]This is energy production. During reheating, this energy is transferred to radiations where the entropy is generated.

where we have assumed a flat space-time $K = 0$, and the subscript $'0'$ denotes the current value of the parameters. This equation reveals a relation $\dot{a}^2 \propto a^{2-3(1+w)}$ which implies the connection between the scale factor $a(t)$ and time t,

- Era dominated by Non-relativistic Matter

$$a(t) \propto t^{2/3}, \tag{2.24}$$

- Era dominated by Relativistic Particles

$$a(t) \propto t^{1/2}, \tag{2.25}$$

- Accordingly, cosmological constant, which means $w = -1$, implies the following relation

$$a(t) \propto \exp(Ht). \tag{2.26}$$

In general, if $p_i = w_i \rho_i$, we can have the equation,

$$\left(\frac{H}{H_0}\right)^2 = \sum_i \Omega_{(i)} \left(\frac{a}{a_0}\right)^{-3(1+w_{(i)})} + \Omega_\kappa \left(\frac{a}{a_0}\right)^{-2}. \tag{2.27}$$

where the dimensionless quantity $\Omega_{(i)} = \frac{8\pi G \rho_0^{(i)}}{3H_0^2}$ describes the ratio of the current energy density and the critical value $\rho_{crit} = 3H_0^2/(8\pi G)$, while $\Omega_\kappa = -\kappa/a_0^2 H_0^2$. By this definition we will have the consistency relation,

$$\sum_i \Omega_{(i)} + \Omega_\kappa = 1, \tag{2.28}$$

From the observational data, we have

- Barionic Matter: $\Omega_b \simeq 0.05$,
- Dark Matter: $\Omega_d \simeq 0.25$,
- Dark Energy (or equivalently the cosmological constant): $\Omega_\Lambda \simeq 0.7$,
- Photons: $\Omega_\gamma \simeq 5 \times 10^{-5}$.

2.3 The Thermal History of the Universe

The thermal history describes the process of the universe evolving from the high temperature and compacted state to the current stage in which the background temperature is 3K and dominated by dark energy. The whole process consists of three stages: Radiation Domination Stage, Matter Domination Stage and Dark energy Domination Stage.

When the background temperature was very high, the universe was filled with high energy particles, some of the lighter ones were relativistic. We denote those particles whose motion is relativistic as "Radiation" while others with non-relativistic properties as "Matter". During radiational era, the relation for energy and temperature is

$$\rho_\gamma \propto g_* T^4 \tag{2.29}$$

where g_* denotes the effective degree of freedom of spin. We adopt natural unit $\hbar = c = k_B = 1$, and the above equation can be rewritten as,

$$g_* = \sum_{\text{i Boson}} g_i \Big(\frac{T_i}{T}\Big)^4 + \frac{7}{8} \sum_{\text{i Fermion}} g_i \Big(\frac{T_i}{T}\Big)^4 \tag{2.30}$$

In the following we will estimate the temperature for the universe. During Radiational era photons obey Planck statistics, therefore the state equation is written as,

$$P_\gamma = \rho_\gamma / 3 \tag{2.31}$$

Applying the conservation law for energy, we can obtain the energy density in this era,

$$\rho_\gamma a^4 = const. \tag{2.32}$$

From this equation we can conclude that the energy enclosed in a comoving sphere is decreasing in an expanding universe.
In a Matter domination era, the energy of universe is dominated by the static energy of the dark and visible matter particles. In this case, the work of the pressure changes just the thermal energy. Therefore by means of conservation law for energy in Eq. (2.19), we have during this era

$$\rho_m a^3 = const. \tag{2.33}$$

This equation presents an invariant quantity which means the matter enclosed in a comoving sphere is preserved as the scale factor a, changes with time t.

Together with the Friedmann equation, we can also estimate the temperature for each era in the universe. Regarding to the early universe which is dominated by Radiation, combing Eq. (2.29) and Eq. (2.32) give,

$$\big(a(t)T\big)^4 \propto const, \tag{2.34}$$

or

$$T \propto a^{-1}(t) \tag{2.35}$$

It means that the decrease of the temperature in the early universe implies an increase in the scale factor, or that the expansion of the Universe results in the drop of the temperature of the universe.

Having known the relation for the temperature, we can understand well the thermal history of the universe.

The birth of Universe General Relativity studies the universe in a manner of classical approach. It implies that if we discuss the time singularity, $t \to 0$, the temperature and the energy density will both approach to infinity. Therefore the theory of General Relativity encounters a singularity problem. To solve it, the gravitational field is regarded as a quantum field just like as treating the ordinary field. However the idea has not yet proven true in experiment though many trials have been under investigation.

Once the hypothesis of quantisation of gravity satisfied or verified, the effect from quantised gravity should not be neglected. By means of dimensional analysis, its effective energy shall be (in natural units),

$$E \sim T \sim \sqrt{1/G} = 10^{19} GeV \tag{2.36}$$

which is the Planck energy, and accordingly there is a Planck time of form

$$t \sim \sqrt{G} = 10^{-43} s \tag{2.37}$$

In general, if the expansion of the universe starts after Planck time, then it is naturally believed that the temperature of the universe is lower than Planck temperature.

Radiational Era

The magnitude of the observed primordial fluctuation reveals that the inflation ends around $T < 10^{16}GeV$, after which the universe enters the reheating era followed by the radiation era.

According to the analysis from the Standard Model (SM) of particle physics, in the very beginning of the Radiational era, the component, "Gas", of the Universe mainly consisted of Quarks, Leptons and gauge bosons, etc. But particle physics theory cannot study properly the physics above the energy level higher than 10^3GeV, and we don't have a working model of Grand Unification Theory (GUT). At temperature $T \sim 10^{15}GeV$, the symmetry in GUT may simultaneously break down to the symmetry in electro-weak theory. While at $T \sim 300GeV$, $SU(2)_L \times U(1)_Y$ symmetry will also break down to $U(1)_{EM}$ in which SM will generate particles with mass. Before the breaking of electro-weak symmetry, supersymmetry may break, however, its mechanism is still under review.

During $10^{-5}s \sim 10^{-4}s$, the chiral symmetry breaks down, and induces color confinement and results in the forming hadrons from quarks. This is the quantum chromodynamics (QCD) phase transition.

Around $T \sim 10MeV$ ($t \sim 0.01s$), protons and neutron form nuclei. This process continues until the reach of temperature around $1MeV$. At this energy level, nuclear physics starts working. The formation of primordial nuclei happens around the time $t = 3 \sim 30min$ after the Big Bang. After the end of nuclei formation, the major components left in the universe at this stage is ${}^2H$ and small amounts of other heavier elements. All those components play a crucial role in studying universe in detail. The abundance of ${}^4He$ is about 1/4 compared to all the baryonic matter, as supported both by the observational data and the theory of Big Bang Nucleousynthesis.

At $T \sim 1MeV$, neutrinos decouple and form the cosmic neutrino background. Electrons and positrons (E-P) which are of mass $0.5MeV$ annihilate into photons. The temperature of decoupled photons is 1.4 times higher than the one before the E-P decoupling. However the spectrum of neutrinos has not yet been found.

Matter Domination Era

At temperatures below $10eV$, the energy level approaches that of atomic physics. About $1eV$ or $t \sim 10^4 yr$, the density of both matter and radiation is equal. Later, the matter dominates the universe. The growth of the primordial anisotropy generated during inflation stage occurs, and the large scale structure (LSS) starts to form.

At $T \sim 0.1eV$ or $t \sim 10^5 yr$, or redshift $z \sim 1100$, atoms form and the decoupling of photons happens. The decoupled photons will travel free in the universe, and their energy spectrum does not change. While the temperature will decrease with the expansion, the Cosmic Background Radiation will form and remain. From the ionization energy of Hydrogen, once the universe is cooled down to $T \sim 13.6eV$, atoms will form. But due to the fact that photons are 1 billion times more numerous than baryons, the atoms will be reionised due to frequent scattering even when the temperature is below of the ionisation temperature $T \sim 13.6eV$.

Up to $t \sim 10^9 yr$, primordial clusters form, and will always evolve with time. They make up a major component of the universe in the Matter Dominated Era.

Dark Energy Era

At about a couple of billion years, the dark energy (DE) starts dominating our universe (given cosmological constant as DE). The present relative density of DE is $\Omega_{\Lambda 0} = 0.73$ and matter $\Omega_{m0} = 0.27$. Also the age of the universe is $t_0 = 13.7Gyr$, it means that our current universe enters a DE dominating era around $0.63t_0$ or 8.3 billion years ago.

2.4 Cosmological Perturbations and Structure Formation

The Cosmological Principle states that the universe is homogeneous and isotropic on scales larger than $100Mpc$. On smaller scales we find that the Universe is filled with non-linear astronomical structures as a results of gravitational collapse from tiny primordial inhomogeneous matter distributions. These primordial fluctuations originate from the quantum fluctuation of scalar fields during inflation stage. In this section we give a brief introduction of this topic.

2.4.1 The Origin of the Primordial Perturbation

Various experiments prove that the universe is highly isotropic and homogeneous at $t \ll 300,000 yrs$. However, the present universe obviously has some anisotropy in structures as follows: Stars ($\delta\rho/\rho \sim 10^{30}$), Galaxies ($\delta\rho/\rho \sim 10^{5}$), Clusters ($\delta\rho/\rho \sim 10 - 10^{3}$), supercluster ($\delta\rho/\rho \sim 1$) and Voids ($\delta\rho/\rho \sim -1$).

Standard cosmological model explains this issue in a broad frame[51, 52, 53, 54]. In the Matter Dominated Era, the primordial density perturbation, which is $\delta\rho/\rho \sim 10^{-5}$, will be enlarged by gravity and evolves finally to the current structures we observe. This will be discussed in the next subsection.

As we mentioned above, the discovery of inflation helps the Big Bang theory win out by solving several severe problems in it and providing a successful explanation on the structure formation. We discuss one of these problems- primordial fluctuation problem as an example to understand how it works.

On the last scatting surface (LSS), the fluctuation between two points will dominate the difference of the gravity potential between these two points, and in turn it gives the temperature of photons.

$$\left(\frac{\delta T}{T}\right)_{\theta} \sim \left(\frac{\delta\rho}{\rho}\right)_{\lambda}, \tag{2.38}$$

We called this effect as Sachs-Wolfe (SW) effect. CMB experiments will give this distribution of temperature in space. And the anisotropy of it can be presented and studied by decomposing into the Spherical functions,

$$\frac{\Delta T}{T}(x_0, \tau_0, \mathbf{n}) = \sum_{\ell m} a_{\ell,m}(x_0) Y_{\ell m}(\mathbf{n}), \tag{2.39}$$

where x_0 and τ_0 denotes our current position and current time, respectively. And $\mathbf{n}$ denotes the direction of observation performed by observers while ℓ is the multipole moment [6]

$$\langle a_{\ell m} a^{*}_{\ell' m'} \rangle = \delta_{\ell,\ell'} \delta_{m,m'} C_{\ell}, \tag{2.40}$$

[6] Equivalently, $C_\ell = \langle |a_{\ell m}|^2 \rangle = \frac{1}{2\ell+1} \sum_{m=-\ell}^{\ell} |a_{\ell m}|^2$.

where C_ℓ is the angular power spectrum of CMB. In the case of homogenous case, C_ℓ is a function of neither x_0 nor of m. But two-point correlation function and C_ℓ have the following relation,

$$\begin{aligned}\left\langle \frac{\delta T(\mathbf{n})}{T}\frac{\delta T(\mathbf{n}')}{T}\right\rangle &= \sum_{\ell\ell' mm'} \langle a_{\ell m} a^*_{\ell' m'}\rangle Y_{\ell m}(\mathbf{n}) Y^*_{\ell' m'}(\mathbf{n}') \\ &= \sum_\ell C_\ell \sum_m Y_{\ell m}(\mathbf{n}) Y^*_{\ell m}(\mathbf{n}') \\ &= \frac{1}{4\pi}\sum_\ell (2\ell+1) C_\ell P_\ell \end{aligned} \tag{2.41}$$

where P_ℓ the Legendre Polynomial of order ℓ.

After considering the LSS, in comoving coordinates, the distance from LSS to the observer is

$$\int_{t_{\rm LS}}^{t_0} \frac{dt}{a} = \int_{\tau_{\rm LS}}^{\tau_0} d\tau = (\tau_0 - \tau_{\rm LS}) \tag{2.42}$$

therefore, the corresponding angular scale on the LSS to which a given comoving distance λ projects is,

$$\theta \simeq \frac{\lambda}{(\tau_0 - \tau_{\rm LS})}, \tag{2.43}$$

where we have neglected the spatial curvature, by assuming a flat universe.

If the length λ is the comoving length of the sound horizon by which the universe evolves to the LSS, it has a value $\lambda \sim c_s \tau_{\rm LS}$, where $c_s \simeq 1/\sqrt{3}$ is the sound speed of photons traveling in plasma. And the corresponding angular scale (or width) is,

$$\theta \simeq c_s \frac{\tau_{\rm LS}}{(\tau_0 - \tau_{\rm LS})} \simeq c_s \frac{\tau_{\rm LS}}{\tau_0}, \tag{2.44}$$

where we have already known $\tau_0 \gg \tau_{\rm LS}$. From the time of decoupling of photons, universe is dominated by matter. We have the relation for scale factor $a \sim T^{-1} \sim t^{2/3} \sim \tau^2$. With $\theta_{\rm HOR}$ which denotes the width of sound horizon on LSS during this era, we can obtain

$$\theta_{\rm HOR} \simeq c_s \left(\frac{T_0}{T_{\rm LS}}\right)^{1/2} \sim 1^\circ, \tag{2.45}$$

where we have adopted $T_{\rm LS} \simeq 0.3$ eV and $T_0 \sim 10^{-13}$ GeV. The width corresponds to a multipole moment $\ell_{\rm HOR}$,

$$\ell_{\rm HOR} = \frac{\pi}{\theta_{\rm HOR}} \simeq 200. \tag{2.46}$$

It also means if two photons with the width larger than $\theta_{\rm HOR}$ (i.e. the corresponding multipole-moment is less than $\ell_{\rm HOR} \sim 200$), they cannot be causally connected.

However, the experimental data from the Cosmic Background Explorer (COBE), the Wilkinson Microwave Anisotropy Probe(WMAP), and the experiments based on the earth and balloons, indicate that on large scales, $\ell \ll 200$, the fluctuation of the temperature in CMB is of amplitude $\delta T/T \sim 10^{-5}$

We find the first peak of the power spectrum is located at $\ell \sim 200$ which equivalently denotes that the patches of multipole moment $\ell_{\rm HOR} \sim 200$ have NO causal connection. However, the photons which come from those patches have a very small anisotropy. And we know that it is impossible to smooth the difference of temperature between two patches which have no causal connection. Therefore this conflict or inconsistency raises the problem of interest – the origin of the Primordial Fluctuations.

However, this primordial problem as well as the many problems of Big Bang (horizon, flatness, entropy, massive particle abundance problems) can be elegantly solved all together if we introduce a dynamical process during which:

- the Universe expands nonadiabaticly
- the increase of physical scale λ must be faster than horizon scale H^{-1}

The first requirement is to solve the entropy and the flatness problem since an nonadiabatic phase is able to provide large entropy we observed today; as to the second requirement, if there has been such a phase that the physical scale λ evolves faster than horizon scale H^{-1}, then the two photons located in no-causal connection areas at LSS ($\lambda > H^{-1}$) could be in causal connection area ($\lambda < H^{-1}$) at an earlier time. Thus the homogeneity and isotropy in scales beyond causal connection at LSS can be explained: the photons in no-causal connection area actually had chance to communicate at a earlier time, therefore have similar temperature.

This second requirement indicates a cosmological stage where $(\frac{\dot{\lambda}}{H^{-1}}) = \ddot{a} > 0$. We define it as a stage of inflation:

$$\text{INFLATION} \iff \ddot{a} > 0$$

As shown in Fig. 2.1(a), assuming that λ denotes the distance between two photons at present, we will find these two photons could not "communicate" (red line lies above green line) since the photons live and travel since decoupling. However, if we assume an inflation stage as in Fig. 2.1(b), then the homogeneity and isotropy on scales beyond causal connection we discussed before can be explained.

Inflation also provides the Universe with seeds for today's inhomogeneous matter distribution on small scales. The physical mechanism is as follows: during Inflation, the energy density of the Universe which is dominated by potential energy of fields or vacuum, keeps almost constant although the Universe is expanding. From Eq. (2.12), this indicates a fixed Hubble constant leading to a fixed horizon H^{-1}[7]. Because microscopic space-time continually being stretched out into macroscopic size, tiny quantum fluctuations of the space-time background were also stretched out. According to the equation of motion of the linear perturbation, the perturbation evolves on smaller scales and becomes frozen when being stretched out of the horizon. Thus inflationary paradigm provides an adiabatic, Gaussian and nearly scale-invariant fluctuation which is consistent with the CMB observations.

When these fluctuations re-enter the horizon at late times, the curvature perturbation functions as the potential wells causing the embedded matters collapse, providing seeds for the cosmic structure that we observed today, which would be amplified by gravitational instability to produce non-linear structures, such as galaxies and clusters which would be briefly introduced in next subsection, Fig.(2.2) depicts the stretch out and re-entery of the primordial fluctuations.

[7]From Eq.(2.26), constant energy density causes an exponential expansion which is so rapid during the time scale we are interested in that the photons hardly traveled any distance.

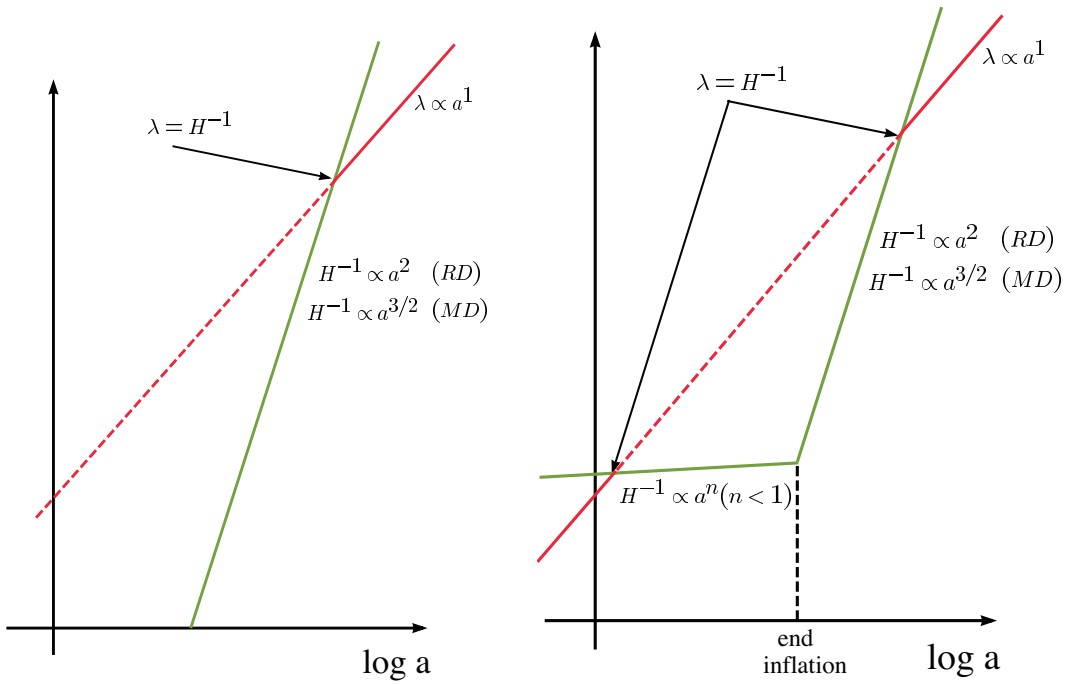

(a) sketch of λ and H^{-1} in thermal Big Bang phase. In this radiation and matter dominated stage, horizon increases faster than physical scale. When two photons are separated by a physical distance $\lambda > H^{-1}$(dashed line region), they do not have a chance to "communicate" or, in other words, beyond causal connection.

(b) sketch of λ and H^{-1} in thermal as well as an additional inflation phase. The added inflation stage happened before thermal Big Bang stage, and, in this stage, the evolution of physical scale is faster than horizon. In this schematic diagram, the horizon is almost fixed (H is constant) corresponding to a exponential space-time expansion.

Figure 2.1: The evolution of physical length λ (red line) and horizon H^{-1} (green line) as a function of the scaler factor a. From this graph we can see that the adding of the inflation stage makes the two photons beyond causal connection having a chance to be correlated with each other.

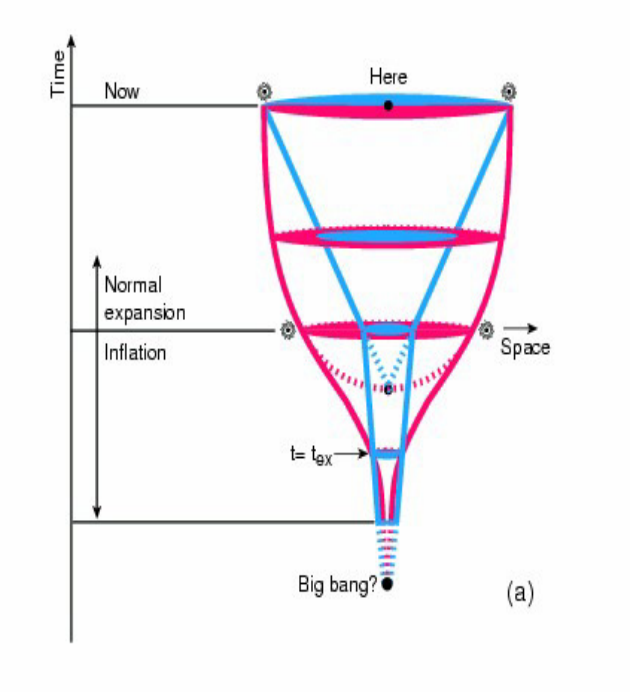

Figure 2.2: The stretching out and re-entering of the primordial fluctuations. The blue line represents the horizonH^{-1} which is almost constant during inflation or increases slowly as in slow roll inflation scenario but constantly increase in normal expansion stage. The red is the wave length λ of the primordial perturbation which originates from quantum fluctuations, being stretched out at $t = t_{ex}$ and reenter the horizon now and would affect future evolution of the Universe.

2.4.2 Primordial Fluctuations to Matter Power Spectrum

Now, Inflation provides a scale invariant Gaussian fluctuation, this means that the Fourier modes of the fluctuation $\delta_{\mathbf{k}}$ does not correlate with other modes. It is convenient to work in Fourier space,

$$\delta_{\mathbf{k}} = \int \delta(\mathbf{x}) e^{-i\mathbf{k}\cdot\mathbf{x}} d^3\mathbf{x}, \tag{2.47}$$

where $\delta(\mathbf{x})$ is the density contrast $\frac{\rho(\mathbf{x})-\overline{\rho}}{\overline{\rho}}$ at position $\mathbf{x}$, $\overline{\rho}$ is the mean density.
Statistical isotropy implies the power spectrum can be described by a scalar function $P(k)$:

$$\langle \delta_{\mathbf{k}} \delta_{\mathbf{k}'} \rangle = (2\pi)^3 P(k) \delta^3(\mathbf{k} - \mathbf{k}'), \tag{2.48}$$

To quantify the amplitude of the fluctuations, we calculate the mass fluctuation within some

volume[51]:

$$\begin{aligned}\left\langle\left(\frac{\delta\rho}{\rho}\right)^2\right\rangle &= \langle\delta^2(\mathbf{x})\rangle = \int\frac{d^3\mathbf{x}}{V}\delta^2(\mathbf{x}) \\ &= \int\frac{d^3\mathbf{x}}{V}\int\frac{d^3\mathbf{k}}{(2\pi)^3}\frac{d^3\mathbf{q}}{(2\pi)^3}\delta_{\mathbf{k}}\delta^*_{\mathbf{q}}e^{i(\mathbf{k}-\mathbf{q})\cdot\mathbf{x}} \\ &\simeq V^{-1}\int\frac{d^3\mathbf{k}}{(2\pi)^3}\left|\delta_k\right|^2 = V^{-1}\int\frac{k^3|\delta_k|^2}{(2\pi^2)}\frac{dk}{k},\end{aligned}$$

The integrand is the dimensionless power spectrum

$$\Delta^2(\mathbf{k}) = \frac{V^{-1}}{2\pi^2}k^3|\delta_k|^2, \tag{2.49}$$

which is the power spectrum popular in the early Universe community. In the large scale structure community, the k^{-3} factor is often added so that it has the dimension k^{-3} [52], i.e. $P(k) = V^{-1}|\delta_k|^2$. In the following, we shall use the dimensional power spectrum $P(k)$. The nearly scale-invariant primordial power spectrum finally leads to a matter power spectrum we observe. The complex cosmic evolution can suppress or enhance the strength of the perturbation spectrum on different scales. The overall effect can be encapsulated in a transfer function $T(k, z)$, and the matter power spectrum at redshift z would be:

$$P(k, z) = P_s(k)T^2(k, z), \tag{2.50}$$

where $P_s(k)$ is the power spectrum of primordial fluctuations. In practice, people have developed several Boltzmann codes to calculate the transfer function, such as CMBFAST [20] and CAMB [21].

As time goes by, the effect of the transfer function will increase ($T(k, z)$ increases as z decreases), causing a lager and lager density perturbation. The region would detach from the background when the density perturbation reaches unity, and non-linear dark matter halo forms.

Chapter 3

Method and Results

The thermal SZ effect has been detected for both individual cluster samples and as an anisotropy signal in the CMB power spectrum [27][28]. On the other hand, the detection of kinetic SZ effect is just getting started. Recently, in anticipation of the coming observational data, the kinetic SZ effect has received considerable attention and aroused widespread interest among cosmologists. There are debates on whether we can use kinetic SZ spectrum to distinguish the dark energy model from their alternatives, such as inhomogeneous universes leading to apparent acceleration. And more and more new papers such as *Observational Consequences of Dark Energy Decay* [55] which look at oriented motion of astro objects trend to discuss the kinetic SZ signal. In this chapter, we calculate the power spectrum of the kinetic SZ effect and determine what percent of the power comes from linear and non-linear parts of matter power P(k).

3.1 The Kinetic SZ Effect

The kinetic SZ effect arises if a large population of free electrons are moving relative to the Hubble flow. In the reference frame of the scattering medium, the CMB radiation appears anisotropic. A small part of the CMB photons scatter with the charged medium (inverse-Compton scattering) and re-isotropize the radiation a little bit. Then, back in the rest frame of the observer the radiation field no longer appears isotropic.

This anisotropy of the scattered photons causes a slight change in the intensity of light

in certain directions. The specific intensity of a radiation field can be described by radio-astronomers in units of brightness temperature $T_{RJ} = \frac{c^2 I_\nu}{2k_B \nu^2}$, where I_ν is intensity ν is frequency of photons. It is an effective temperature. The spectrum of the CMB is no longer a black body spectrum but with a particular frequency structure. This property is extremely important in cosmological observations. We use this characteristic frequency structure to decide if a certain type of anisotropy is due to the kinetic SZ effect or some other anisotropy source such as the thermal SZ effect.

It's easy to imagine that to increase the anisotropy caused by the scattering, we can either increase the anisotropy of each scattered photon or increase the number of photon with anisotropy. The former corresponds to an increase in the flow velocity, while the latter corresponds to increasing the scattering probability (optical depth), which is equivalent to an increase in the density of free-electrons, since the cross section of Compton scattering is constant. They have equal weights. Thus we can guess that the kSZ effect is proportional to the product of peculiar velocity and charge density.

In Compton scattering, only the line of sight direction component of the velocity has an effect on the intensity we observe, the cross sky component has no contribution. Sunyaev and Zel'dovich, in 1972, gave the result that the radiation temperature decrease in the kinematic effect is [26]:

$$\frac{\Delta T}{T} \approx -\tau_e \frac{\upsilon_z}{c} \ . \tag{3.1}$$

This formula also provides a method for measuring line of sight component[1] of the peculiar velocity of an object at large distance[2]. Therefore, $\upsilon_z = \hat{\upsilon} \cdot \hat{\mathbf{n}}$ is the component of peculiar velocity of the scattering atmosphere along the line of sight and τ_e is the optical depth from the observer to the scatterer:

$$\tau_e = \int n_e \sigma_T dl \tag{3.2}$$

where σ_T is the Thomson cross section.

[1]The cross-sky component of the peculiar velocity can be measured via gravitational lensing

[2]Provided that the kinetic and thermal effects can be separated, as they have different spectral properties

The probability that the photon we observed was scattered once is $\tau_e e^{-\tau_e}$, thus the fractional temperature distortion due to the kinetic SZ effect along the line-of-sight unit vector $\hat{n}$ is

$$\frac{\Delta T}{T}(\hat{\mathbf{n}}) = \frac{1}{c}\int dl\, e^{-\tau} n_e \sigma_T\, \hat{\mathbf{n}}\cdot\boldsymbol{v} \tag{3.3}$$

The kinetic SZ effect probes the density weighted peculiar velocity of ionized gas up to the epoch of reionization, and is a sensitive measure of the reionization history. We assume that the Universe suddenly ionized at $z = z_{\rm rei}$ and remain completely ionized after that. We can write

$$\frac{\Delta T}{\mathrm{T}}(\hat{\mathbf{n}}) = \frac{\sigma_T}{c}\int_0^{z_{\rm rei}} \frac{dx}{dz}\frac{dz}{(1+z)}\exp(-\tau(z)) n_e(z)\mathbf{v}\cdot\hat{\mathbf{n}} \tag{3.4}$$

where the Thomson optical depth τ as a function of z is

$$\tau(z) = \sigma_T \int_0^z \frac{\bar{n}_e(z')}{1+z'}\frac{dx}{dz'}dz' \tag{3.5}$$

and where $\bar{n}_e$ is the proper mean electron density,

$$\bar{n}_e(z) = \frac{\chi\Omega_b\rho_c(1+z)^3}{\mu_e m_p} \tag{3.6}$$

its relation with the electron density is $n_e = \bar{n}_e\,(1+\delta)$, χ is the ionization fraction, Ω_b is today's baryon density parameter, ρ_c is the critical density, and m_p is the proton mass.

3.2 Statistical Method

The angular two-point correlation function of the CMB anisotropy $C(\theta)$ is

$$C(\theta) = \left\langle \frac{\Delta T}{T}(\hat{\boldsymbol{n}}_1)\frac{\Delta T}{T}(\hat{\boldsymbol{n}}_2)\right\rangle = \sum_{\mathrm{l}=0}^{\infty}\frac{(2\mathrm{l}+1)}{4\pi}C_\ell\,\mathcal{P}_\ell\,, \tag{3.7}$$

where C_ℓ is the angular power spectrum, and $\mathcal{P}_\ell(\cos\theta) = \mathcal{P}_\ell(\hat{\boldsymbol{n}}_1\cdot\hat{\boldsymbol{n}}_2)$ are the Legendre polynomials. For $\ell \gg 1$, the C_ℓ can be calculated using Limber's approximation,

$$C_\ell \;=\; \frac{8\pi^2}{(2\ell+1)^3}\left(\frac{\sigma_T\rho_{\mathrm{g},0}}{\mu_e m_p c}\right)^2\int_0^{z_{rei}}(1+z)^4\chi^2\Delta_B^2(\ell/x,z)\exp\big(-2\tau(z)\big)x\frac{dx}{dz}dz \tag{3.8}$$

where $k = \ell/x$. Vishniac [56] first calculated the expression for Δ_B^2

$$\begin{aligned}\Delta_B^2(k) \;&=\; \frac{k^3}{2\pi^2}\int\frac{d^3k'}{(2\pi)^3}\Big[(1-\mu^2)P_{\delta\delta}(|\mathbf{k}-\mathbf{k}'|)P_{vv}(k') \\ &\quad -\frac{(1-\mu^2)k'}{|\mathbf{k}-\mathbf{k}'|}P_{\delta v}(|\mathbf{k}-\mathbf{k}'|)P_{\delta v}(k')\Big]\;,\end{aligned} \tag{3.9}$$

where μ is $cos\theta$, in which θ is the angle between k and k', and $P_{\delta\delta}$ and P_{vv} are the linear theory density and velocity power spectra, and $P_{\delta v}$ is the density-velocity cross spectrum.

The continuity equation relates the density and velocity power spectra: $\tilde{\mathbf{v}}(\mathbf{k}) = i\hat{\mathbf{k}}(f\dot{a}/k)\tilde{\delta}(\mathbf{k})$, where $f = d\log D/d\log a$ and D is the linear growth factor. Therefore,

$$P_{vv}(k) = \left(\frac{f\dot{a}}{k}\right)^2 P_{\delta\delta}(k) \; ; \quad P_{\delta v}(k) = \left(\frac{f\dot{a}}{k}\right) P_{\delta\delta}(k) \quad . \tag{3.10}$$

Plugging these into Eq. (3.9), we obtain

$$\Delta^2_B(k) = \frac{k^3}{2\pi^2}\dot{a}^2 f^2 \int \frac{d^3k'}{(2\pi)^3} P_{\delta\delta}(|\mathbf{k}-\mathbf{k}'|)P_{\delta\delta}(k')I(k,k') \quad , \tag{3.11}$$

where

$$I(k,k') = \frac{k(k-2k'\mu)(1-\mu^2)}{k'^2(k^2+k'^2-2kk'\mu)} \; .$$

These formulae describe the linear part of the kinetic SZ effect which is also called Ostriker-Vishniac effect[25, 57].

3.3 Results

We get the linear and non-linear matter power spectrum from CAMB and use it to calculate the kinetic SZ power spectrum $l(l+1)C_l/2\pi$. Our main purpose is to investigate the impact of density fluctuations on the kinetic SZ temperature fluctuation, connecting the matter power of the Universe with the KSZ power spectrum we can observe.

The values of some parameters we use hereafter are: $z_{rei} = 10$, $Y_p = 0.24$, $\chi = 0.86$(i.e.,$N_{H_e} = 0$), $\mu_e = 1.14$, $\Omega_{DM} = 0.727$, $\Omega_m = 0.2735$, $\Omega_b = 0.0455$, $\Omega_r = 0$, $h = 0.704$, $\sigma_8 = 0.7935$.

3.3.1 The Impact of Reionization

One of the many properties of the kinetic SZ effect is that it is sensitive to the details of reionization history which is hard to confine by other observations. This is because astronomical signals or apparent brightness drops as $1/(1+z)^2$ when probing high redshift events, and

only very bright objects such as supernova and quasars[3] can do the work. However, the kinetic SZ effect is redshift-independent, because it is the CMB photons that are observed and the temperature variation fraction does not change. Therefore, kinetic SZ effect provides a unique probe of very large scale structures and extremely important in studying reionization.

We assume the Universe suddenly ionized at $z = z_{\rm rei}$ and remain completely ionized after that. We get Fig. (3.2), the kinetic SZ power with different value of $z_{\rm rei}$.

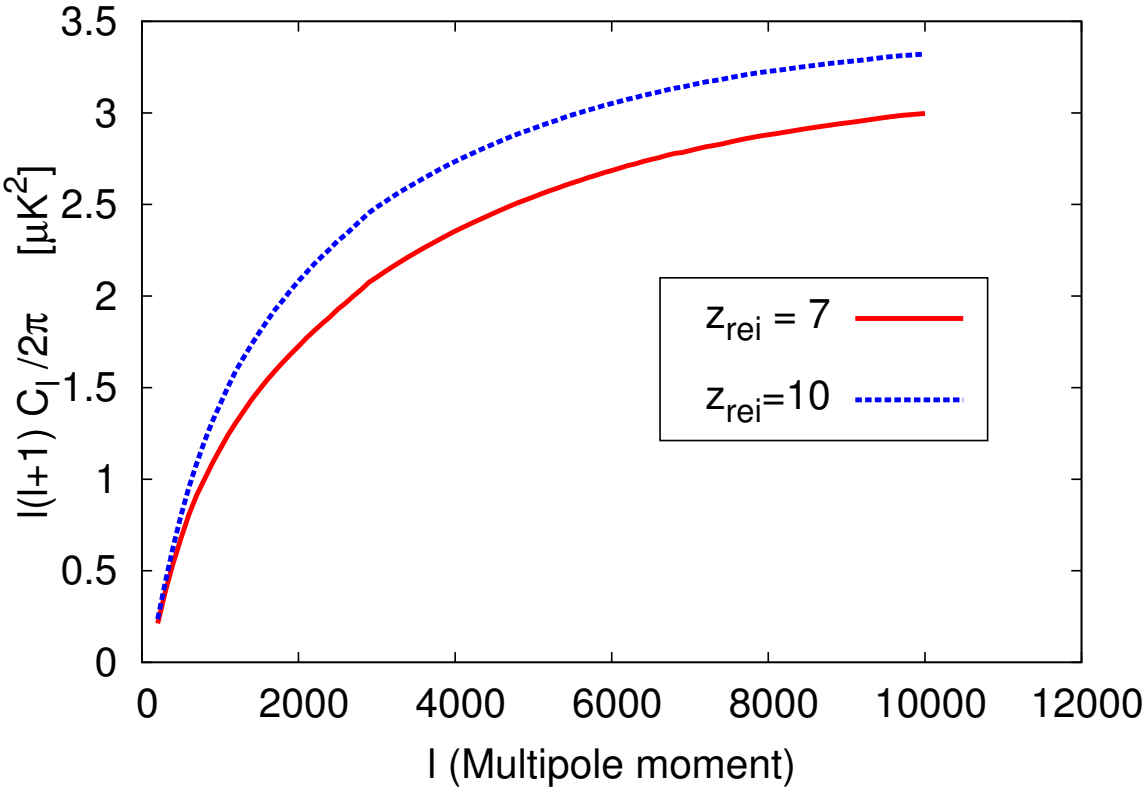

Figure 3.1: The kinetic power spectrum. The solid and dot line corresponds to $z_{\rm rei}$ equal to 7 and 10 respectively. This figure indicates that the earlier the reionization happened, a lager kSZ effect would be observed today. The kSZ is sensitive to z_{rei}.

We find that the earlier reionization begins, the higher kinetic SZ effects will be as we expected. This is because the fraction of temperature changes of kinetic SZ is proportional to

[3] From the absence of the Gunn-Peterson effect in quasar absorption spectrum, we know reionization must be complete by $z \sim 5$[58, 59].

the density-weighted-velocity integrated along the line of sight, while the density integral along line of sight is sensitive to the reionization. A longer duration of reionization leads to a higher kSZ effect.

Besides, we also noticed that the differences between these two plots quickly increases from 0 to $0.4\mu K^2$ at around $l = 1100$ and then remains almost constant making it different from other the effects that we will looking into where this difference tends to increase with l.

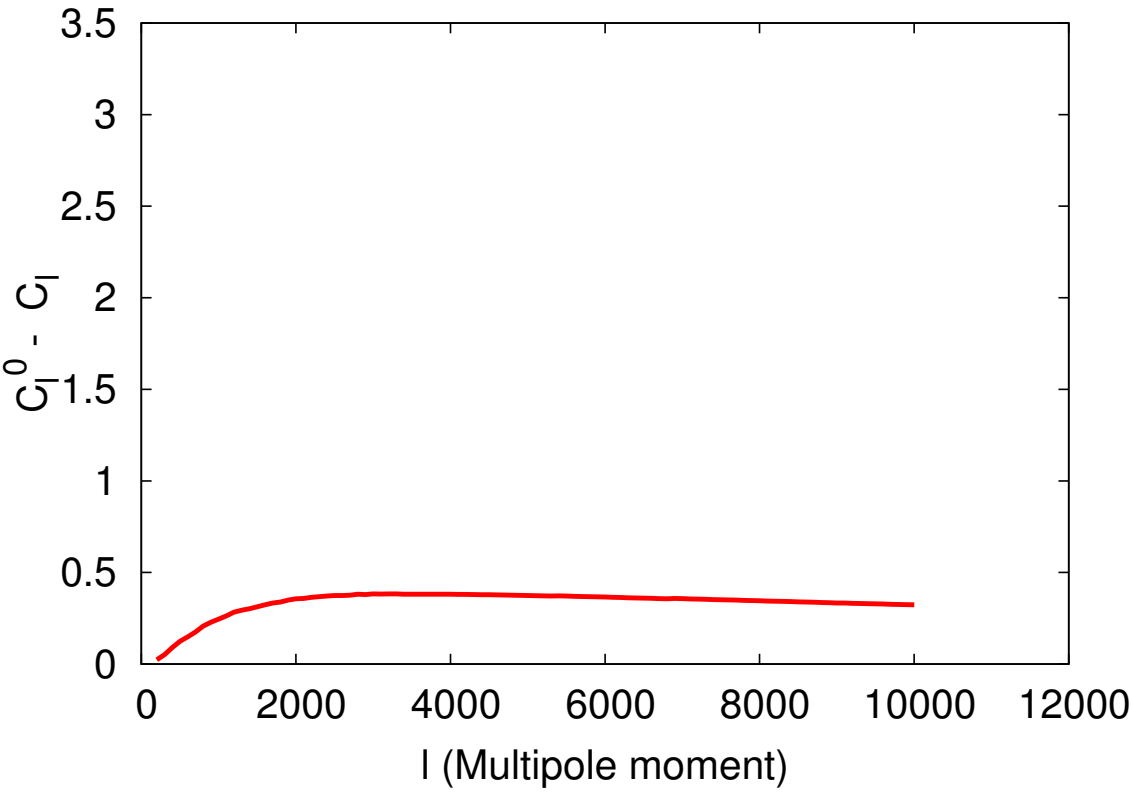

Figure 3.2: The amplitude difference between $z_{rei} = 10$ and $z_{rei} = 7$ quickly goes up to $0.4\mu K$ and remains almost constant indicating Z_{rei} affects kSZ globally.

Theoretically, this can be interpreted as follows: the reionization history's effects on kSZ is global; it uniformly affects the kSZ on all the scales except the largest ones. On the other hand, the other physical effects contributing to the kSZ that we will be looking at are all

local, foreground effects, and will turn out to give an increasing kSZ temperature difference[4] as l increases.

3.3.2 Linear and Non-linear Contributions

As we mentioned in the beginning of this chapter, the kinetic SZ effect is proportional to the free-electron density and the bulk peculiar velocity along the line of light. These informations are embedded in Eq. (5.2) where they come via the product of the two density power spectra $P_{\delta\delta}(|\mathbf{k}-\mathbf{k}'|)$ and $P_{\delta\delta}(k')$, since we have utilized the continuity equation Eq. 3.13 expressing the bulk velocity spectrum in terms of the density power spectrum and the correlation is embedded in the I(k,k') function.

To understand this correlation, we first define a function

$$C(k) = \int \frac{d^3k'}{(2\pi)^3} P_{\delta\delta}(|\mathbf{k}-\mathbf{k}'|) P_{\delta\delta}(k') I(k,k') \tag{3.12}$$

which is the integral part of Δ_B^2 in Eq. (5.2), and plot $C(k)$ in Fig. (3.3).
From Fig. (3.3), we can tell that the contribution mainly comes from $k < 0.4h^{-1}MPC$ which includes the linear ($k < 0.2$) and mildly non-linear regime. This agrees with our expectation, because the bulk velocity is induced by the potential well around it, and the potential arises mainly from the large scale (linear) density perturbations because of the $1/k^2$ suppression in Eq. (3.13). The mildly non-linear structure also contributes by providing a relatively large free-electron density so that the CMB photons can scatter with it.

To make this more intuitive, we want to determine what percentage of the power of temperature fluctuation comes from linear and non-linear parts of matter power $P(k)$. We calculate up to which ℓ of C_ℓ^{ksz} contribution from $k > 0.2$ of $P_{\delta\delta}(k)$ is less than 10%. We denote the power spectrum contributed from linear velocity power spectrum ($P_{vv}$with $k < 0.2$)[5] as C_ℓ^*, thus C_ℓ^* is part of the total kinetic SZ effect (denoted as C_ℓ^0). We compare C_ℓ^* with C_ℓ^0 and find $\ell_* \simeq 3930$ at which the deviation $\frac{C_\ell^0 - C_\ell^*}{C_\ell^*} \geq 10\%$. This deviation goes up as ℓ increases

[4]Here, the difference is the difference of kSZ temperature between when we include certain physical effect (non-linear structures, baryonic gas pressure, cooling and star formation) and when we do not include it.

[5]we set $P_{vv} = 0$ when $k > 0.2$ but use $P_{\delta\delta}$ with $k \in [0, \infty]$.

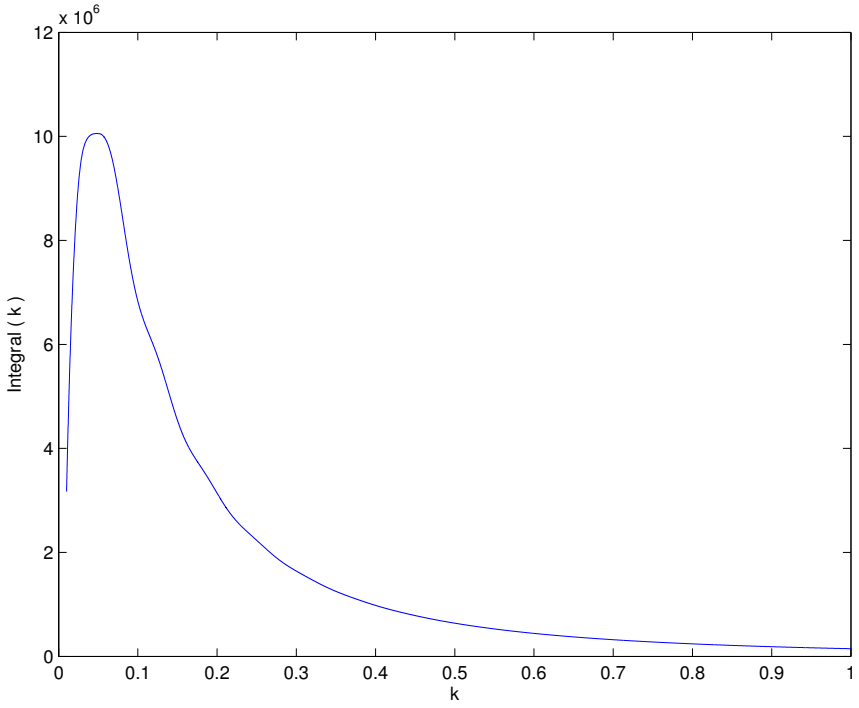

Figure 3.3: $C(k)$. Note that $C(k)$ quickly increase to its maximal in linear region, then quickly goes down in the mild non-linear region.

which is reasonable according to our previous analysis.

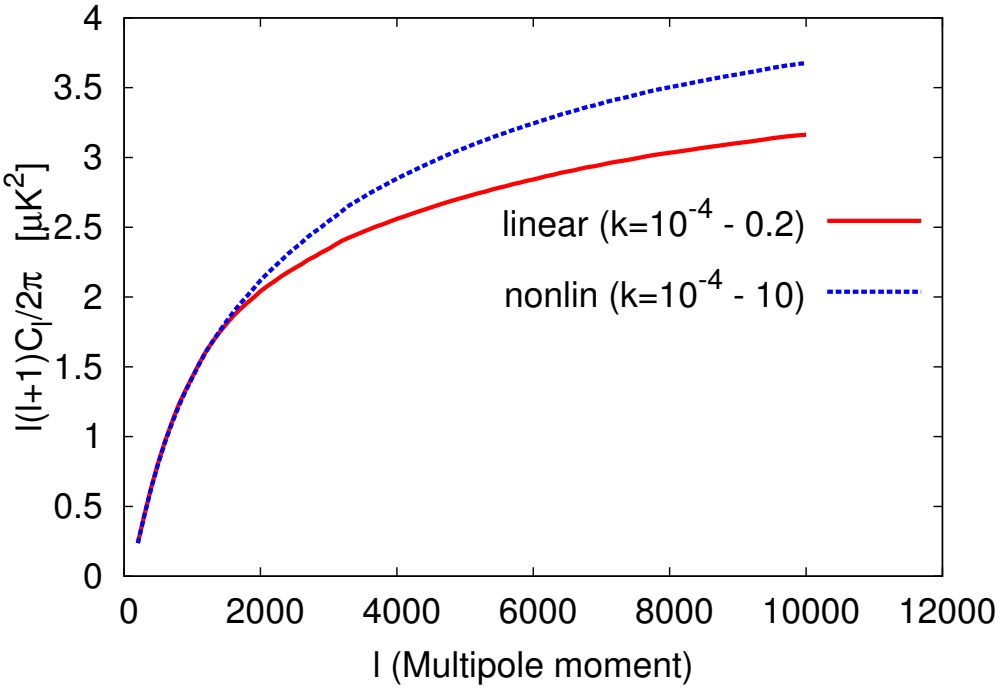

Figure 3.4: C_ℓ^* (solid red) and C_ℓ^0 (dot blue). C_ℓ^* counts only the linear contribution of P_{vv}, while C_ℓ^0 holds the whole contribution (both linear and non-linear part) of P_{vv}. The result shows that the difference is small indicating that the non-linear part of the velocity power's contribution can be neglected.

Fig. (3.5) draws the percentage deviation between non-linear-cutoffed P_{vv} and whole P_{vv} contribution. It shows that the deviation (cutoff-ed nonlinear P_{vv} contribution) is not large, and it changes dramatically from $l = 1800$ to $l = 4000$ and then becoming stable.

Besides, since the free-electron density is provided mainly by the non-linear density distribution, we can imagine that if we eliminate the non-linear part density power spectrum $P_{\delta\delta}$ [6] rather than P_{vv}, the power spectrum of temperature fluctuation will be changed more significantly, and the experiment supports this expectation.

[6] We can achieve this by setting $P_{\delta\delta} = 0$ when $k > 0.2$ but using P_{vv} with $k \in [0, \infty]$.

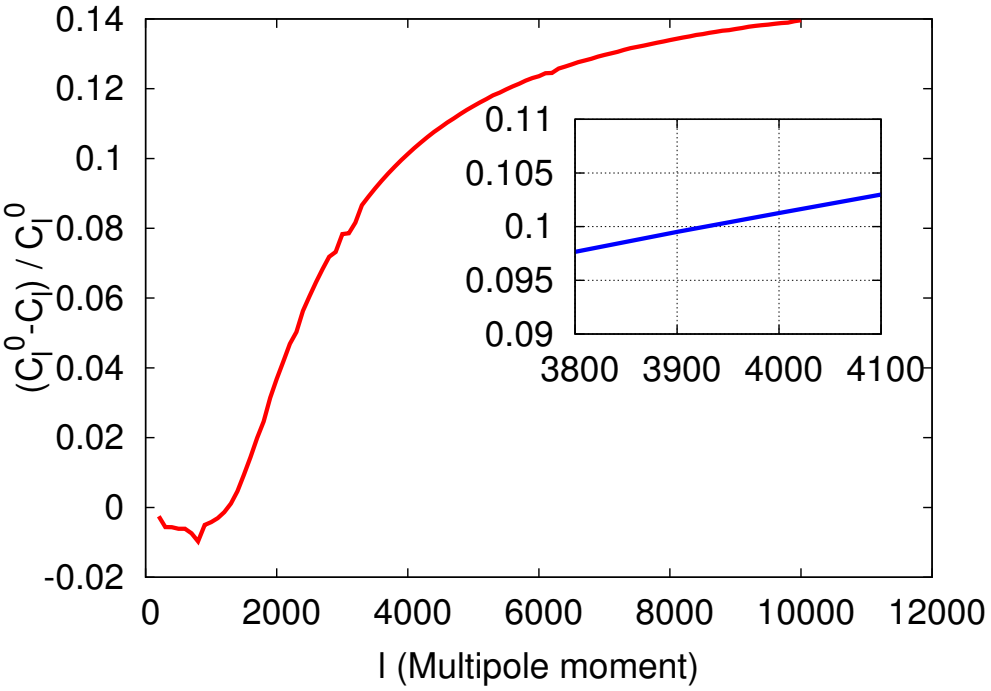

Figure 3.5: The deviation of C_ℓ^* with C_ℓ^0 goes up as ℓ increases. In the small box we mark the point of 0.1 crossing: untill around $l = 3930$ the difference rises up to 10%.

3.3.3 Going Beyond Linear Perturbation Theory

In Section 3.2, we listed the formula for calculating C_l^{kSZ}. This formula was deduced from linear perturbation theory. This linear part of the kinetic SZ effect is known as the Ostriker-Vishniac effect.

However, while linear perturbation theory explains the large structure of our Universe, it fails when the density contrast reaches order unity. And the cosmic structures we observe in kinetic SZ effect are super clusters, clusters and even galaxies which have density contrast larger than unity. Therefore, theoretically, we can not use Eq. (3.8) directly to calculate C_ℓ by simply plugin a non-linear matter power spectra $P_{\delta\delta}^{NL}$ into Eq. (5.2). These equations are deduced from linear theory.

However, the kinetic SZ effect is determined by the density weighted peculiar velocity. This density and velocity field information is encoded in the product of two matter power $P_{\delta\delta}(|\mathbf{k}-\mathbf{k}'|)$ and $P_{\delta\delta}(k')$. We have transferred the velocity power spectrum P_{vv} into $P_{\delta\delta}(k')$ by using the continuity equation:

$$P_{vv}(k) = \left(\frac{f\dot{a}}{k}\right)^2 P_{\delta\delta}(k) \; ; \tag{3.13}$$

Besides, based on our analysis and experiments in last subsections, we know that the bulk velocity arise mainly from the linear regime because of the $1/k^2$ suppression [7], in other words, the non-linear evolution in the density field do not have a significant effect on velocity modes. Non-linear contributions to the kinetic SZ effect therefore come mostly from $P_{\delta\delta}(k)$. Therefore, Wayne Hu[60] suggested that, to include the impact of non-linear structure formation, one can simply replace the linear theory matter power spectrum $P_{\delta\delta}$ with non-linear matter power spectrum$P_{\delta\delta}^{\rm NL}$,

$$\Delta_B^2(k) = \frac{k^3}{2\pi^2}\dot{a}^2 f^2 \int \frac{d^3k'}{(2\pi)^3} P_{\delta\delta}^{\rm NL}(|\mathbf{k}-\mathbf{k}'|) P_{\delta\delta}(k') I(k,k') \tag{3.14}$$

We go beyond linear theory and study the impact of non-linear modification of matter power on kinetic SZ temperature fluctuation. The CAMB code not only can calculate linear perturbations but also provides HaloFit subroutine for non-linear matter power. We take

[7] Studies suggested that in the ΛCDM model, half the contributions to v_{rms}^2 comes from scales $k < 0.07 h Mpc^{-1}$[61].

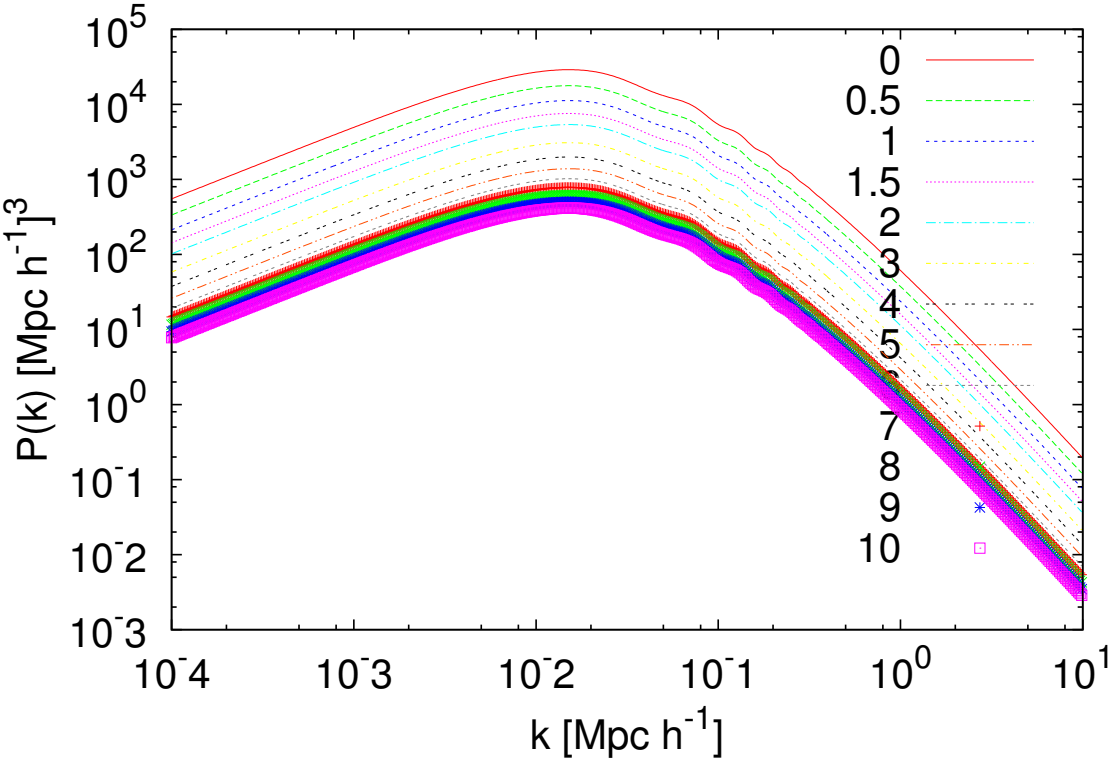

Figure 3.6: The linear matter power spectrum at different redshift between 0 to 10. As shown in this graph, matter power increases with time.

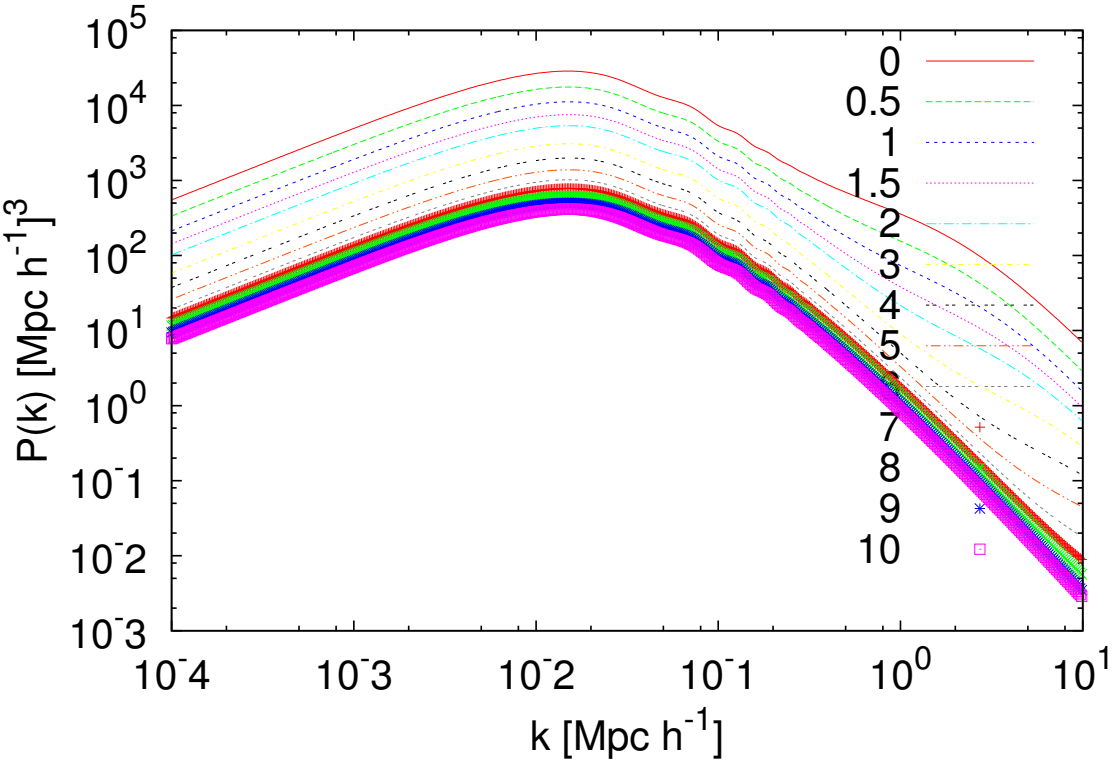

Figure 3.7: The non-linear matter power spectrum at different redshift.

advantage of that, and the matter power we used is shown in Fig. (3.6 3.7). It is a collection of $P(k)$ at redshift z ranging from 0 to z_{rei} (here $r_{rei} = 10$). This collection contains the information about the environment through which the CMB photons were passing through and interacting with at that epoch. The kSZ effect we are looking for is an integral of these historical contributions slice by slice all the way up to the beginning of reionization.

The KSZ power spectrum is plotted in Fig. (3.9), where C_ℓ^{NL} is the power spectrum when HaloFit modification is considered and C_ℓ^L is the result we got when using the original matter power calculated from the linear perturbation theory.

The result shows that the Halo fit non-linear modification has a bigger impact on the C_ℓ than including the non-linear part of the velocity power. The non-linearity increases the kinetic SZ power spectrum one tenth at $l \sim 790$ and increase it more and more on even smaller scales.

We also noticed that one property that makes the Ostriker-Vishniac effect different from the other effects we are interested in is that it reaches its peak very soon at $\ell \sim 2300$, while other effects do not even have a peak. This property reveals that the maximal contribution of linear density fluctuation comes from scales at $\ell \sim 2300$, which corresponds to 0.08 degree angle on the sky.

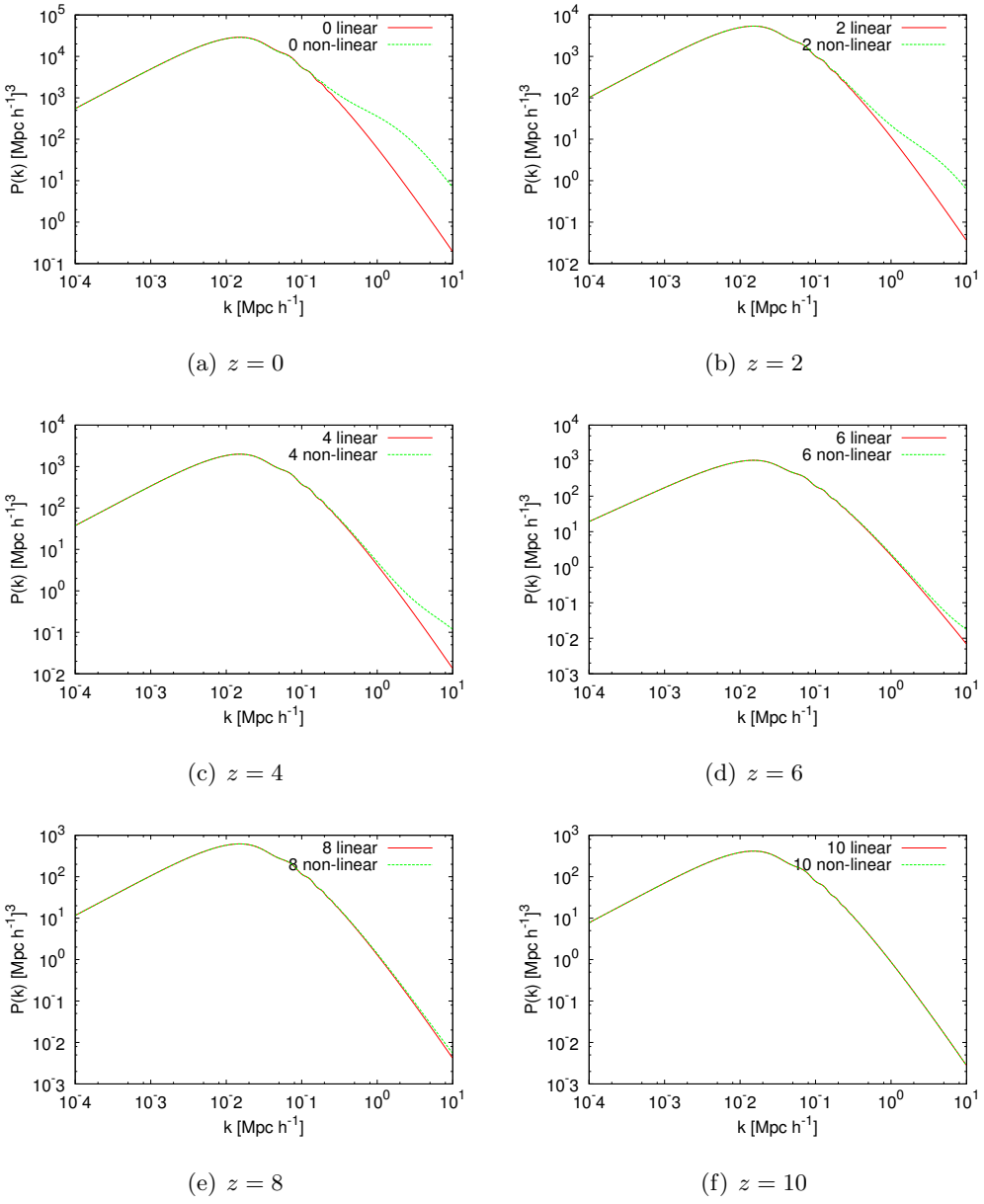

(a) $z = 0$ (b) $z = 2$

(c) $z = 4$ (d) $z = 6$

(e) $z = 8$ (f) $z = 10$

Figure 3.8: The growth of the non-linear matter power spectra. The red line represents the linear power and the green represents the non-linear power. At $z = 10$ the linear and non-linear power superposition to each other. At $z = 8$ the non-linear spectrum starts to have an enhancement in small scale region and this enhancement is getting larger and larger as the Universe expands.

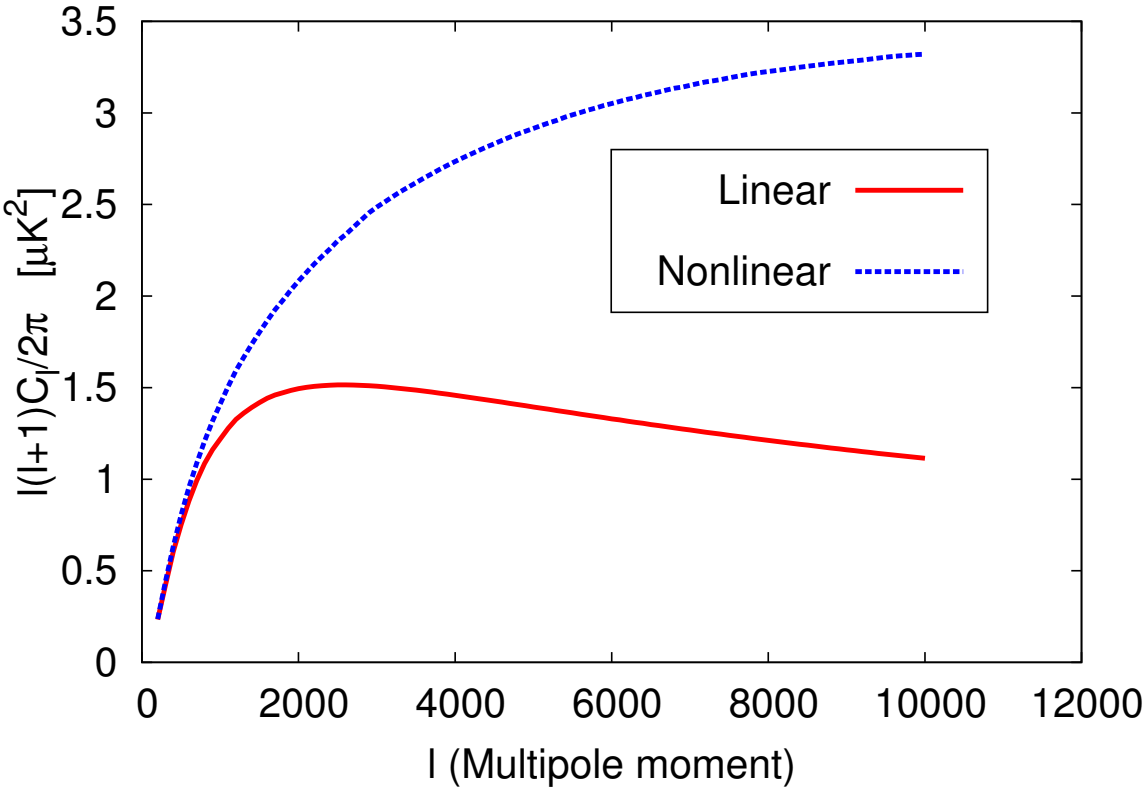

Figure 3.9: $\ell^2 C_\ell^*/2\pi$ and $\ell^2 C_\ell^0/2\pi$ represents linear (red) and non-linear (blue) kinetic SZ power spectrum respectively.

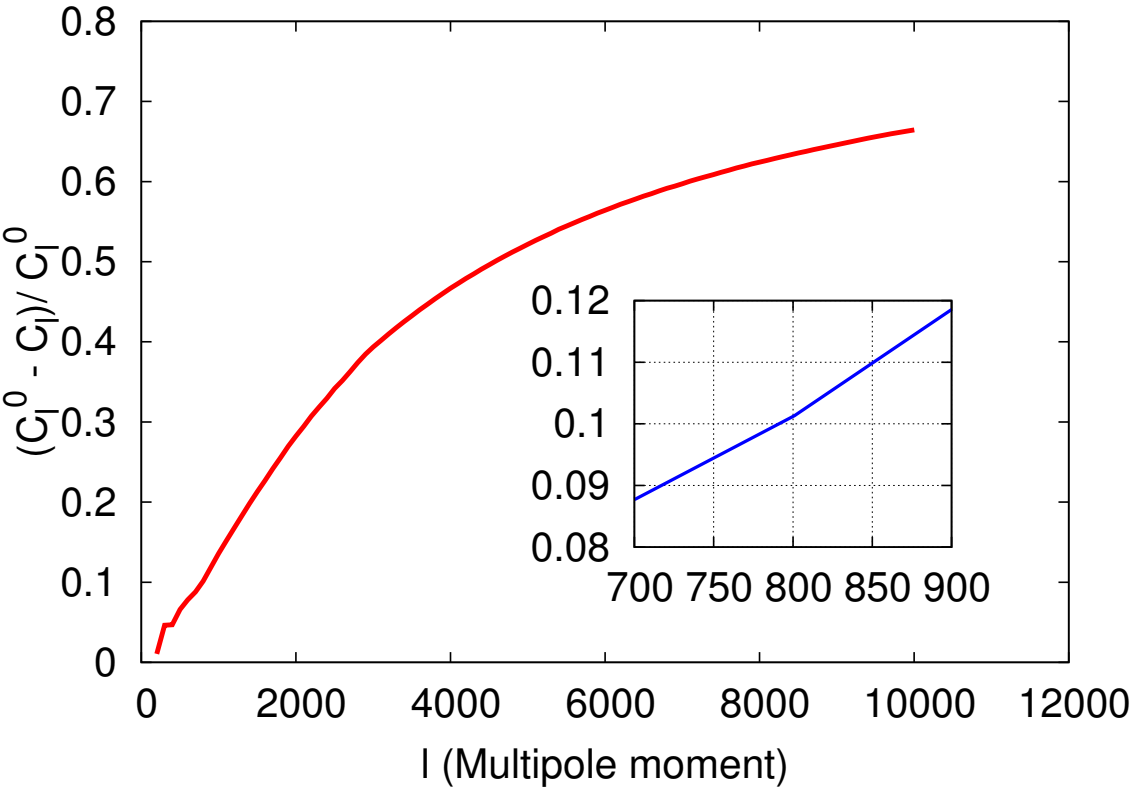

Figure 3.10: The deviation of C_ℓ^* with respect to C_ℓ^0. The large difference indicating the non-linear astronomy structures have a large contribution on kinetic SZ effect.

Chapter 4

Baryonic Effects

In the structure formation theory, Cold Dark Matter decouples earlier than baryons and starts to fall into the potential wells created by the quantum fluctuations during the inflation stage. Baryons are subdominant and they trace the distribution of dark matter after they decouple from radiation later.

The final distribution of dark matter halos can be significantly different from that of baryons because the interactions they are involved in are different. Rudd et al.[62] found that baryonic processes significantly alter predictions for the matter power spectrum relative to models that include only gravitational interactions. They indicate that the physics governing the non-linear evolution of the baryonic component could be important for forecasts of the constraining power of future surveys if scales $\ell > 1000$ are included. Thus, we explore the effects of baryonic processes in this chapter.

4.1 The Baryonic Gas Pressure

Weakly interacting massive particle (WIMP) is the most widely discussed Cold Dark Matter candidate. Compared with baryons, WIMP is obviously a very simple particle. It is supposed to be stable, classic, massive and very weakly interacting (probably only interacts via gravity). Therefore it is easy to simulate the evolution of dark matter which is also the dominant energy budget of all the matter. As for the baryons, because they follow the dark matter because of the gravity, people tend to assume $\delta_b = \delta_{DM}$. However, this is not true

on all scales.

Baryons are not as simple as WIMPs. Baryon particles can have different kinds of charges and interact with each other. They are less massive and can have relatively large velocity. As an example, the thermal pressure between baryons would erase fluctuations on small scales, therefore we have $\delta_b < \delta_{DM}$ on very small scales.

4.1.1 The Window Function

In the previous Chapter, the matter power we used was the matter power of dark matter, but the kinetic SZ effect comes from the interaction of CMB photons with baryon gases, thus in order to predict the kSZ power spectrum accurately, we need to use the matter power of baryons rather than dark matter to do the calculation. We can get the baryon matter power P_{gas} by multiplying the matter power P_{DM} with window function $W(k)$

$$P_{gas}(k,z) = W^2(k,z)P_{DM}(k,z) \ . \tag{4.1}$$

Since the effect of baryon thermal pressure is erasing fluctuations on small scale, we can expect $W^2 \simeq 1$ on large scales (when k is small) and $W^2 < 1$ on small scales (k is large). The analytical expression for the window function is [65]

$$W(k,z) = \frac{1}{2}[exp(-\frac{k^2}{k_f^2}) + \frac{1}{[1+4(\frac{k}{k_f})^2]^{1/4}}] \tag{4.2}$$

where the characteristic filter scale k_f is given by

$$\frac{1}{k_f^2} = \frac{1}{D(t)}\int_0^t a^2(t')dt' \frac{\ddot{D}(t') + 2H(t')\dot{D}(t')}{k_J^2(t')} \int_{t'}^t \frac{dt''}{a^2(t'')} \tag{4.3}$$

where, k_J is the Jean's scale

$$K_J(t) = \frac{a}{c_S(t)}\sqrt{4\pi G\rho_m(t)} \tag{4.4}$$

and ρ_m is the mean matter density and c_S is the mean sound speed at t.

We draw the window function at different redshifts in Fig. 4.1.

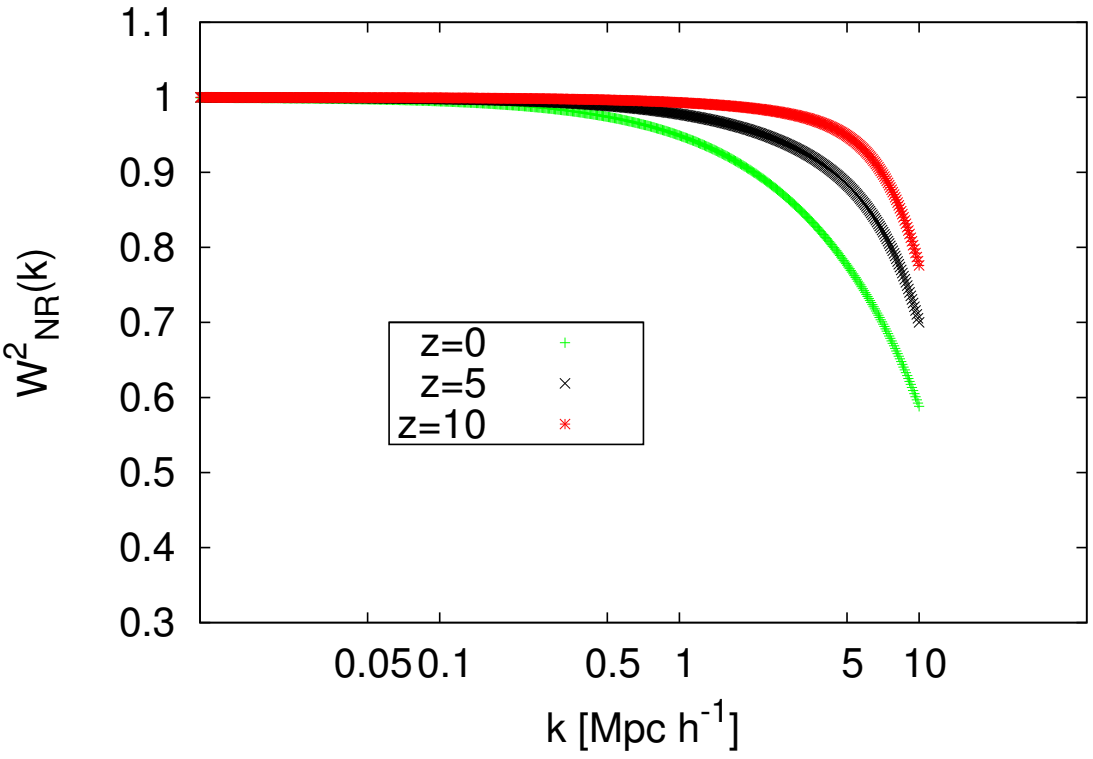

Figure 4.1: Plot of $W^2(k,z)$ at redshifts $z = 0, 5, 10$. Thermal pressure erase δ on small scales and will not affect matter power on large scales, thus W^2 approaches to 1 at small k and then goes down at large k.

4.1.2 kSZ Power Spectrum with Gas Pressure

Gas pressure resists baryon gases collapsing on smaller scales. Because of this suppression of matter power on small scales, we can expect a suppression of C_l^{kSZ} at large l. We do the calculation and plot Fig (4.2) as well as Fig (4.3):

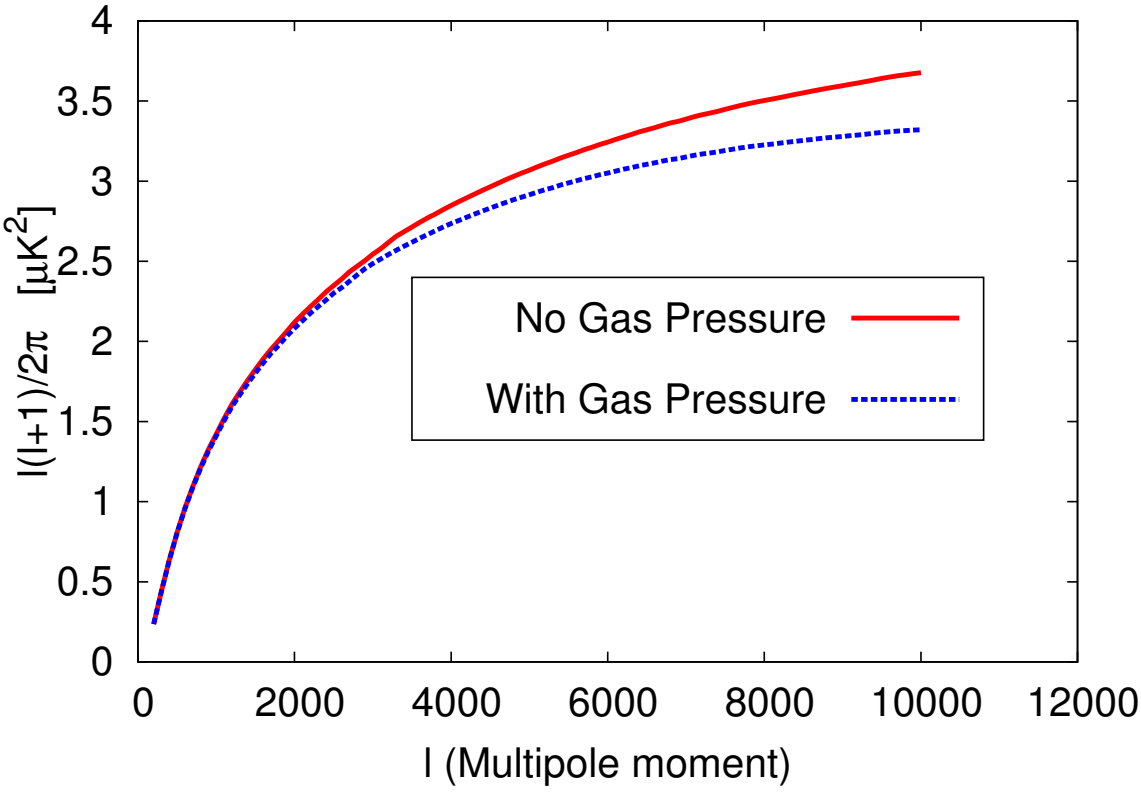

Figure 4.2: The kSZ effect with and without the baryonic gas pressure. This graph shows that the contribution of gas pressure on kSZ power spectrum is to lower its amplitude a little bit. The modification is not as significant as non-linear structure effect or reionization history.

The results is consistent with our expectation, the thermal pressure of baryons decrease the kSZ effect, we find this can cause a $0.1\mu K$ change at $l = 4000$.

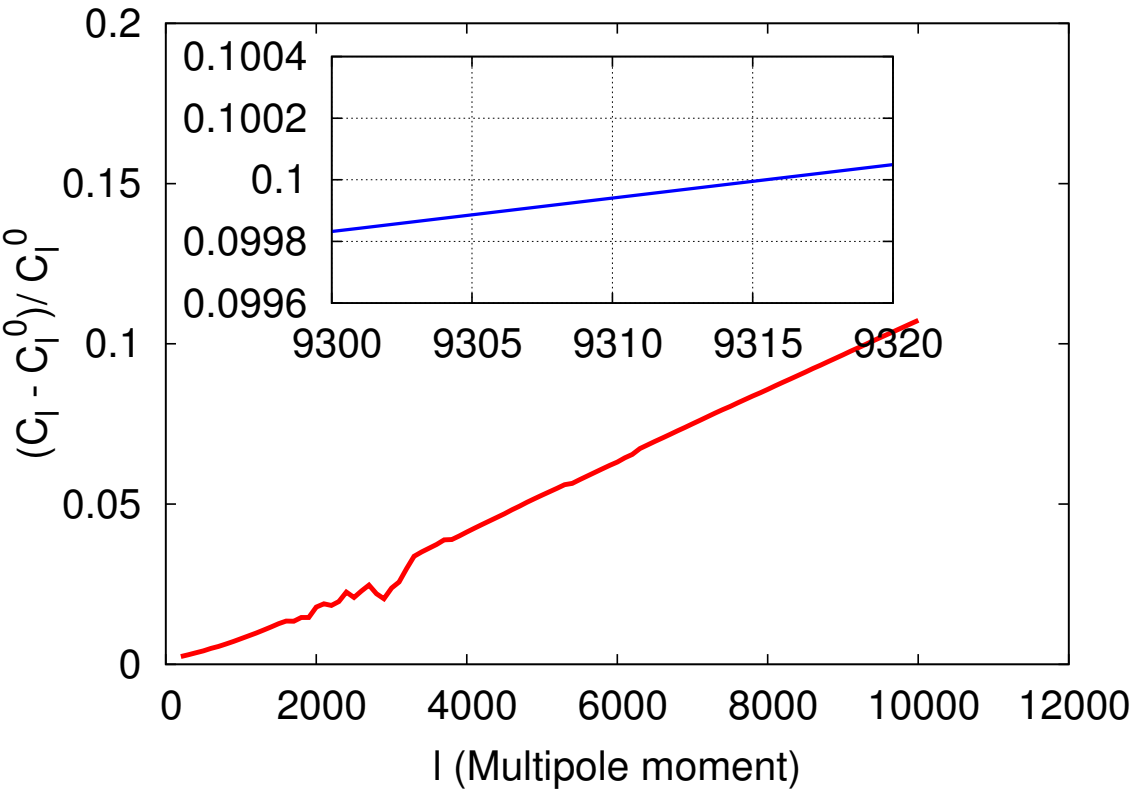

Figure 4.3: The contribution of gas pressure on kSZ is not significant. The deviation increases as l goes up, and when $l \simeq 9316$ the percentage deviation reaches 10%.

4.2 The Baryonic Cooling and Star Formation

Besides the thermal pressure effect discussed in the last section, there are other baryons effects that can have an impact on the matter power spectrum such as radial cooling and star formation. And the changes of matter power will have an impact on the kSZ effect which is the integral effect. To calculate the kSZ effect with high accuracy, in this section we discuss the impact of cooling and star formation.

4.2.1 The CSF Matter Power Spectrum

Rudd et al. [62] find that radiative cooling of the baryonic component, star formation and feedback precesses have a large impact on the power spectrum. This modification can be modeled by multiplying the original gravity-only non-linear power spectrum by a ratio of NFW profiles. We use P_{CSF} to represent the matter power spectra with cooling and star formation and P_{DMO} for the matter power with dark matter only:

$$P_{CSF}(k) \approx P_{DMO}(k)\left[\frac{\lambda(R_{vir}k/c_2, c_2)}{\lambda(R_{vir}k/c_1, c_1)}\right]^2 \tag{4.5}$$

This NFW profile is unity on scales larger than the typical scales of halos $k \lesssim R_{vir}^{-1}$ and differs from unity at higher wavenumbers. The concentration c_1 represents the halos in a typical dark matter simulation, and a second concentration c_2 represents the effective concentrations of the mass profiles of halos with baryonic cooling and galaxy formation included. The analytic expression is given in [61]

$$\begin{aligned}\lambda(\eta; c) = \frac{1}{f_{NFW}(c)}\Bigg\{ &\sin(\eta)[Si([1+c]\eta) - Si(\eta)] \\ &+ \cos(\eta)[Ci([1+c]\eta) - Ci(\eta)] - \frac{\sin(\eta c)}{[1+c]\eta}\Bigg\},\end{aligned} \tag{4.6}$$

where,

$$f_{NFW}(x) = \ln(1+x) - x/(1+x) \tag{4.7}$$

c is the halo concentration, $\eta = kR_{vir}/c$, R_{vir} is the halo virial radius, and $Si(x)$ and $Ci(x)$ are the sine and cosine integrals. From these analytical expressions, we get P_{CSF} in Fig. 4.6

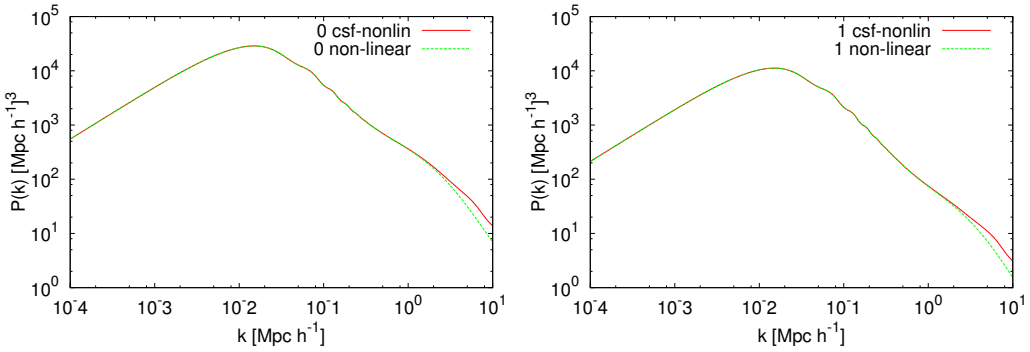

(a) $z = 0$

(b) $z = 1$

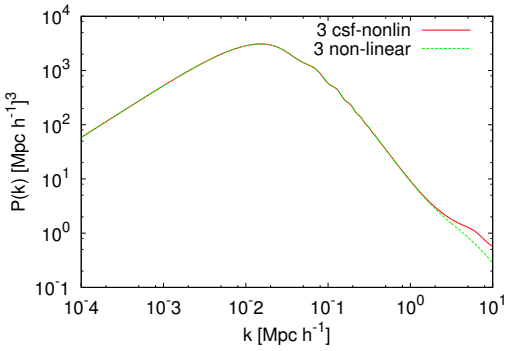

(c) $z = 3$

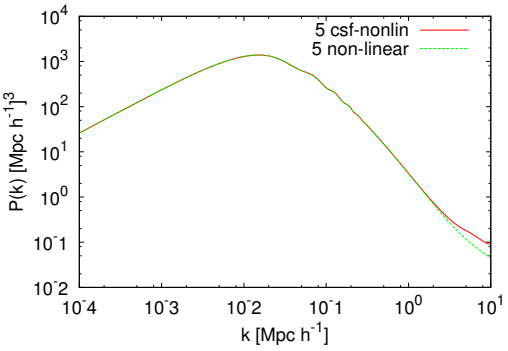

(d) $z = 5$

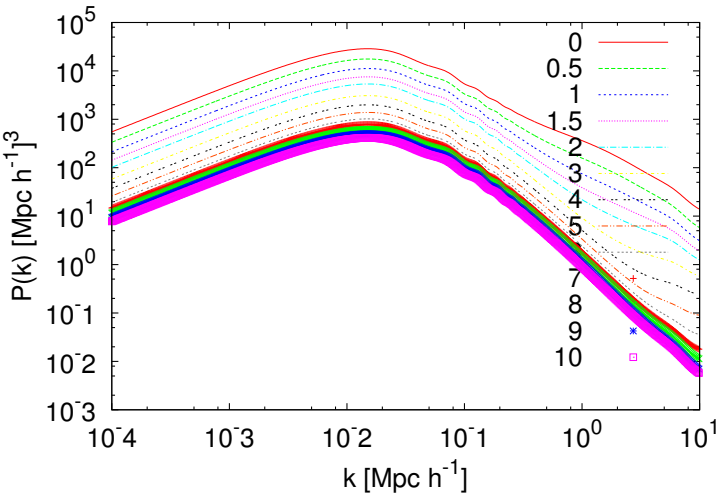

(e) P_{CSF} at different z

Figure 4.4: $P_{CSF}(k)$ and $P_{DMO}(k)$. We use parameters: $R_{vir} = 1.1h^{-1}Mpc$, $c_1 = 5$, $c_2 = 1.7c_1$, which is the typical value for halos at redshift $z \sim 1$. Here we compared P_{CSF} (red) with P_{DMO} (blue) at several redshifts, and we can tell that cooling and star formation enhances the matter power spectrum on small scales (large k), from which we can infer that the kSZ effect probably would be enhanced.

The figure shows that cooling and star formation changes the matter power on small scales a lot (note that it is a loglog plot). It increases the power on scales $10^0 < k < 10^1$.

4.2.2 The CSF KSZ Power Spectrum

We also calculate the C_ℓ^{CSF} using $P_{CSF}(k, z)$ which is plotted in Fig. 4.4(e). This calculation is a rough one – for instance, the parameters c_1, c_2 come from simulation and they should be functions of redshift. However, because there's no detailed information in literature, we use $c_1 = 5$, $c_2 = 1.7c_1$ on all the redshifts to get a result which is not very accurate. From this figure, we can tell that the baryon cooling and star formation do have a significant impact on kinetic SZ power spectrum. They change the magnitude and the shape of the curve by strongly lifting the curve on very small scales.

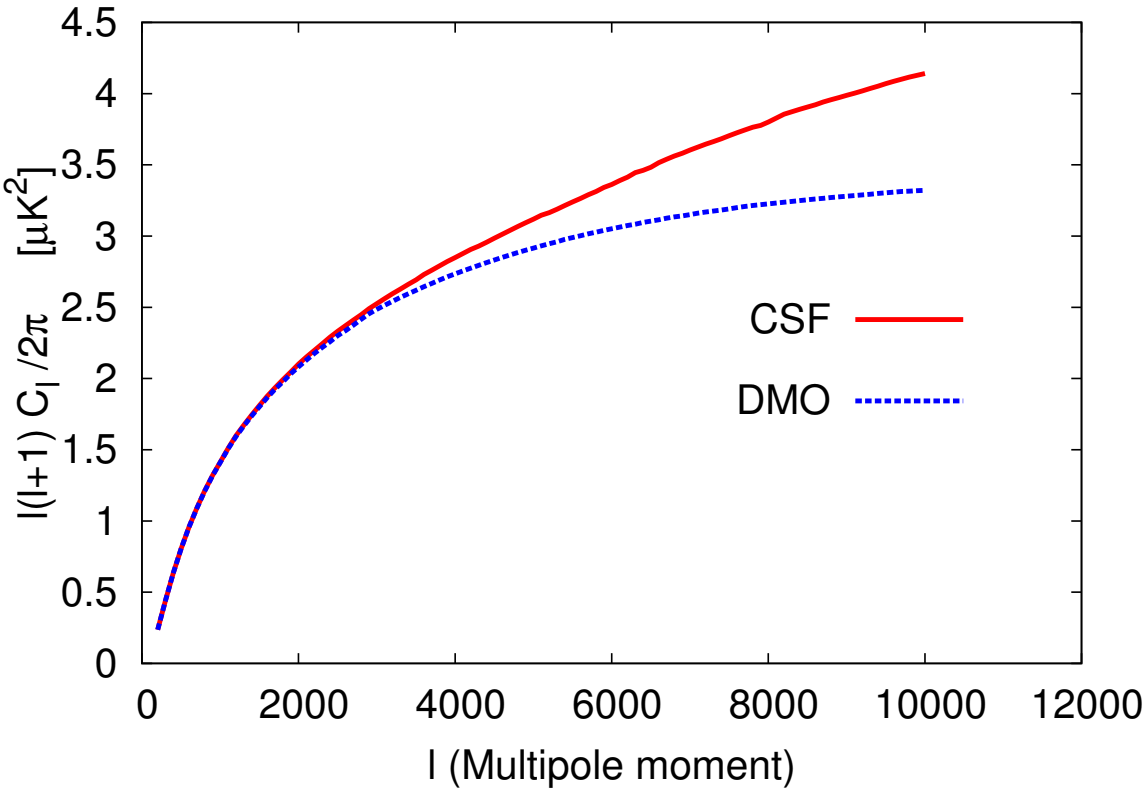

Figure 4.5: Prediction of kinetic SZ power spectrum from different matter power: $P_{CSF}(k)$, $P_{DMO}(k)$. The dot blue line, $P_{\mathbf{DMO}}(k)$(**D**ark **M**atter **O**nly), corresponds to matter power including non-linear modification; The solid red line, $P_{\mathbf{CSF}}(k)$(**C**ooling and **S**tar **F**ormation), corresponds to the matter power including the baryonic processes.

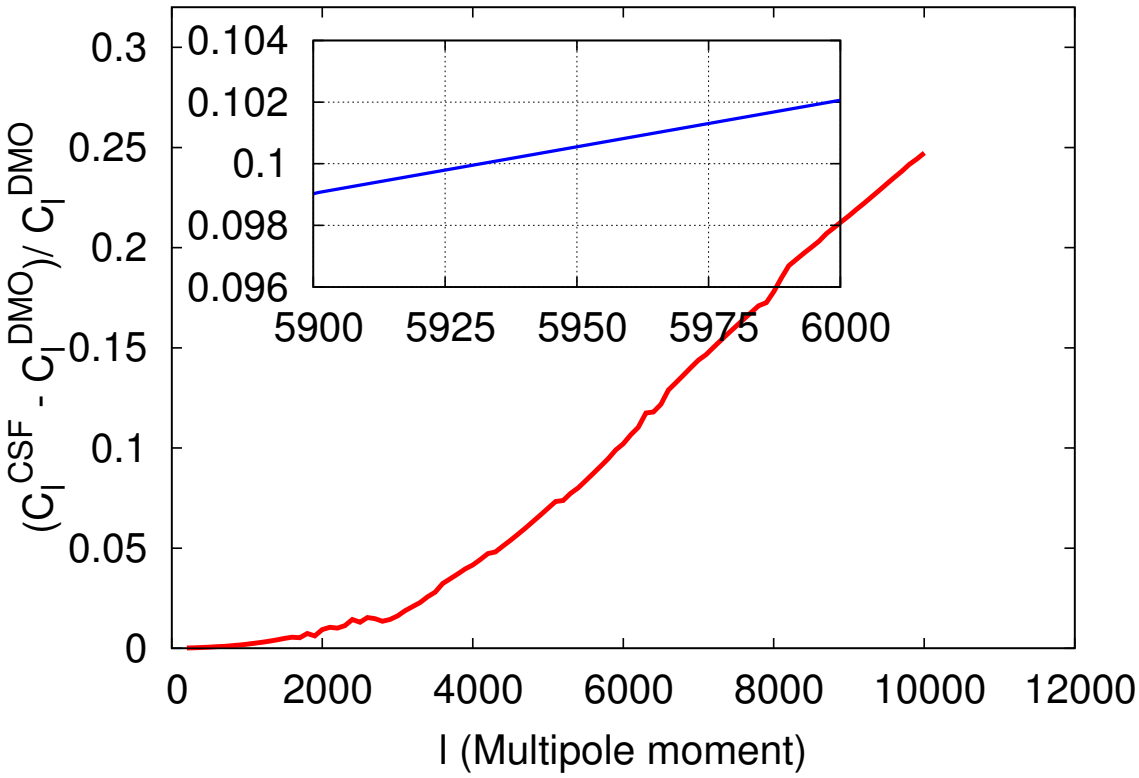

Figure 4.6: A special character for cooling and star formation effect is that its contribution on kSZ increase significantly as l increases. We can see the deviation increases faster and faster, it reaches 10% at $l = 5930$.

Chapter 5

Conclusions, Outlook and Current Observations

The kinetic Sunyaev-Zeldovich effect is an unique way of detecting very large scale physics. It is redshift-independent, so the signal does not diminish. It can be used to detect the peculiar velocity of certain cosmic structures such as clusters, super clusters or galaxies, thus is widely and effectively applied to a lot of interesting physics ideas involving large-scale flows. The kinetic SZ effect is getting more and more popular in past years. The thermal SZ effect has been detected both for individual galaxies and statically, but the kinetic SZ effect hasn't. There are several ground-based arcminute-scale observational projects being build or just starting release data such as the South Pole Telescope (SPT)[63] and Atacama Cosmology Telescope (ACT)[64]. The kinetic SZ effect is promising and worth to explore.

5.1 Conclusions

The kinetic SZ effect arises if the scattering medium is moving relative to the Hubble flow. The fraction of temperature changes of kinetic SZ in certain direction of the sky is proportional to the density-weighted-velocity integrated along the line of sight. After calculating the power spectrum of kSZ, we find that kSZ is sensitive to the details of reionization because the density integral along line of sight depends on it. A longer duration of reionization corresponds to a higher kSZ effect.

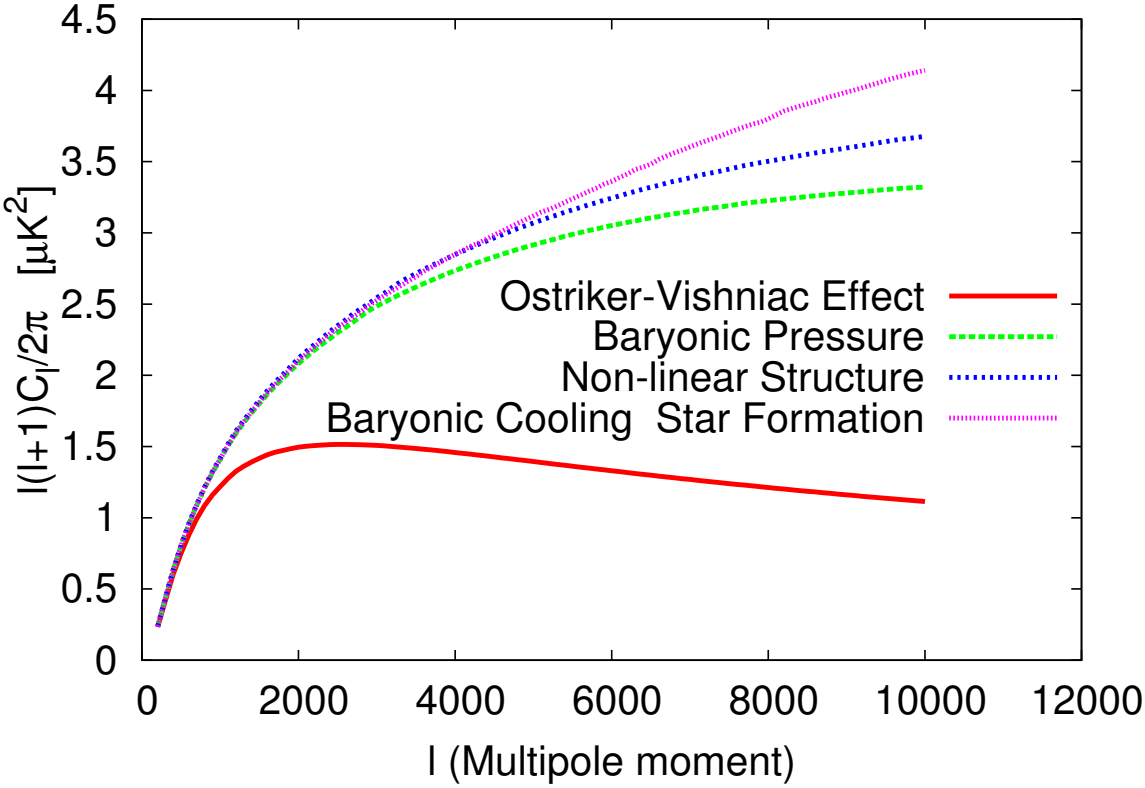

Figure 5.1: A brief summary of the kinetic power spectrum.

The peculiar velocity of a cosmic object is induced by the potential wells around it. On small scales, these potential wells come from the matter distributed around it, while on very large scales, the potential well is formed by the curvature perturbation of the space. On large scales, matter hasn't had enough time to cluster, and large scale flow might happen causing kSZ effect. Our results shows that up to $\ell \sim 3930$ the non-linear velocity fluctuations contribute under 10% of the total kSZ power spectrum. We go beyond the linear perturbation theory, using non-linear density power spectrum $P_{\delta\delta}^{NL}$ to get kSZ power spectrum and compare it with linear density power spectrum case. We find the 10% deviation happens at $\ell \sim 790$. To make accurate prediction of kSZ, we need to consider baryonic effects such as thermal pressure, which proved will decrease kSZ slightly. There are also suggestions that if some baryonic processes are considered, especially when the radial directing cooling and star formation are included, the kSZ power spectrum will be changed significantly. We

calculate the matter power $P_{CSF}(k)$ and confirmed this results. Fig. (5.1)

5.2 Outlook

The kinetic SZ effect has two major advantages: detecting very large scale structures and probing large scale flows. The large structures together would create potential wells around them and wonder within this potential field. We believe this scenario makes the kinetic SZ effect a very good candidate in testing gravity. It is of interests to explore the gravity models via kinetic SZ effects. As an example, we can test f(R) model with the help of the code MGCAMB[66].

Under modified gravity models, the electromagnetic action (Compton scattering) will not be affected, thus the formula for calculating C_ℓ^{kSZ} is the same:

$$C_\ell = \frac{8\pi^2}{(2\ell+1)^3}\left(\frac{\sigma_T \rho_{\mathrm{g},0}}{\mu_e m_p c}\right)^2 \int_0^{z_{rei}} (1+z)^4 \chi^2 \Delta_B^2(\ell/x, z) \exp\big(-2\tau(z)\big) x \frac{dx}{dz} dz \qquad (5.1)$$

$$\Delta_B^2(k) = \frac{k^3}{2\pi^2}\dot{a}^2 f^2 \int \frac{d^3k'}{(2\pi)^3} P_{\delta\delta}^{NL}(|\mathbf{k}-\mathbf{k}'|) P_{\delta\delta}(k') I(k,k') \ , \qquad (5.2)$$

But we need to find all the terms that can be affected by gravity model and replace them with new ones. MGCAMB can do most of the work. We can directly get the linear matter power $P_{\delta\delta}(k)$, Hubble parameter $H(z)$[1]. MGCAMB dose not provide the linear growth factor f, instead it provides $\Delta(k,a)$, and:

$$D(k,a) = \frac{\Delta(k,a)}{\Delta(k,1)} \qquad (5.3)$$

$$f = \frac{d\log D}{d\log a} \qquad (5.4)$$

Till now, the only missing link is the non-linear matter power $P_{\delta\delta}^{NL}$ which must be found in numerical simulations.

[1] for calculating comoving distance in Eq. (5.1)

5.3 Current Observations

Several ground-based telescopes are working on detecting very high resolution ($2000 < l < 10000$) cosmic microwave background anisotropies. The observed angular power spectrum C_l at this scales is a combination of signals from the primary CMB anisotropy, thermal and kinetic SZ effects, radio galaxies and cosmic infrared background. The kSZ contribution can be discriminated from other signals' when a multi-frequency observation is available.

A two years' three-frequency observation from the South Pole Telescope(SPT) sets an upper limit on the kinetic SZ power: at $l = 3000$ the CSF homogeneous kSZ power is less than $2.8\mu K^2$ at 95% confidence[67]. Our results in Fig. (5.1) shows that the kSZ power at $l = 3000$ (around $2.5\mu K^2$) is right below this upper limit. Different kSZ models we discussed have almost the same power at this scale, and thus can not be discriminated yet. The differences will be relevant, however, for future CMB experiments with improved sensitivity.

Bibliography

[1] http://www2.aao.gov.au/2dFGRS/

[2] http://www.sdss.org

[3] http://lambda.gsfc.nasa.gov/product/cobe/

[4] http://map.gsfc.nasa.gov/

[5] http://www.rssd.esa.int/index.php?project=PLANCK

[6] S. Cole et al., MNRAS.362 (2005) 505.

[7] M. Tegmark et al. ApJ.606 (2004) 702.

[8] D. Eisenstein et al. ApJ. 633 (2005) 560.

[9] D. H. Spergel et al., ApJS.148 (2003) 175-194.

[10] D. N. Spergel et al., ApJS, 170 (2007) 377.

[11] E. Komatsu et al., ApJS. 180 (2009) 330.

[12] The Planck Collaboration, 2005, *'The Scientific Programme of Planck'*, eds. G. Efstathiou, C. Lawrence, and J. Tauber, ESA-SCI(2005), ESA Publications.

[13] C. Reichardt et al. ApJ. 694 (2009) 1200.

[14] H. T. Nguyen. et al., Proc. SPIE, 7020 (2008) 70201F.

[15] J. A. Rubino-Martin et al., arXiv: 0810.314; http://www.iac.es/project/cmb/quijote/.

[16] http://bolo.berkeley.edu/POLARBEAR/index.html.

[17] D. Samtleben, arXiv: 0802.2657; http://quiet.uchicago.edu/.

[18] http://groups.physics.umn.edu/cosmology/ebex/index.html.

[19] B. P. Crill, et al., arXiv:0807.1548.

[20] U. Seljak and M. Zaldarriaga, ApJ 469 (1996) 437.

[21] http://camb.info; A. Lewis, A. Challinor and A. Lasenby, ApJ, 538 (2000) 473.

[22] R. K. Sachs and A. M. Wolfe, Astrophys. J. **147**, 73 (1967) [Gen. Rel. Grav. **39**, 1929 (2007)].

[23] M.J. Rees and D.W. Sciama, Nature 217 511 (1968).

[24] Melia. Fulvio, The Galactic Supermassive Black Hole. Princeton University Press (2007)

[25] J. P. Ostriker and E. T. Vishniac, Nature (ISSN 0028-0836), vol. 322, Aug. 28, 1986, p. 804.

[26] Sunyaev RA, Zeldovich YB. 1972. Comments Astrophys. Space Phys. 4:17378

[27] M. BIRKINSHAW, S. F. GULL & H. HARDEBECK Nature 309, 34 - 35 (03 May 1984); doi:10.1038/309034a0

[28] Myers, A. D.; et al. (2004). "Evidence for an Extended SZ Effect in WMAP Data". Monthly Notices of the Royal Astronomical Society 347 (4): L67L72.

[29] Alpher, R.A.; Bethe, H.; Gamow, G. (1948). "The Origin of Chemical Elements". Physical Review 73 (7): 803. doi:10.1103/PhysRev.73.803

[30] Hoyle, F. (1948). "A New Model for the Expanding Universe". Monthly Notices of the Royal Astronomical Society 108: 372.

[31] Misner, Charles W.; Coley, A A; Ellis, G F R; Hancock, M (1968). "The isotropy of the universe". Astrophysical Journal 151 (2): 431. doi:10.1088/0264-9381/15/2/008

[32] Misner, Charles; Thorne, Kip S. and Wheeler, John Archibald (1973). Gravitation. San Francisco: W. H. Freeman. pp. 489490, 525526. ISBN 0-7167-0344-0.

[33] Weinberg, Steven (1971). Gravitation and Cosmology. John Wiley. pp. 740, 815. ISBN 0-471-92567-5.

[34] Dicke, Robert H. (1970). Gravitation and the Universe. Philadelphia: American Philosopical Society.

[35] Dicke, Robert H.; P. J. E. Peebles (1979). "The big bang cosmology enigmas and nostrums". In ed. S. W. Hawking and W. Israel. General Relativity: an Einstein Centenary Survey. Cambridge University Press.

[36] Doroshkevich, A. G.; Novikov, I.D. (1964). "Mean Density of Radiation in the Metagalaxy and Certain Problems in Relativistic Cosmology". Soviet Physics Doklady 9 (23): 4292. doi:10.1021/es990537g

[37] SLAC seminar, "10-35 seconds after the Big Bang", 23rd January, 1980. see Guth (1997), pg 186

[38] Guth, Alan H. (1981). "Inflationary universe: A possible solution to the horizon and flatness problems" (PDF). Physical Review D 23 (2): 347356. Bibcode 1981PhRvD..23..347G. doi:10.1103/PhysRevD.23.347

[39] A. D. Linde, "Quantum cosmology and the structure of inflationary universe," gr-qc/9508019.

[40] Khoury, Justin; Burt A. Ovrut, Paul J. Steinhardt, Neil Turok (28 Nov 2001). "Ekpyrotic universe: Colliding branes and the origin of the hot big bang". Physical Review D 64 (12): 123522. arXiv:hep-th/0103239. doi:10.1103/PhysRevD.64.123522.

[41] Steinhardt, Paul J.; Neil Turok (24 May 2002). "Cosmic evolution in a cyclic universe". Physical Review D 65 (12): 126003. arXiv:hep-th/0111098. doi:10.1103/PhysRevD.65.126003

[42] E. W. Kolb and M. S. Turner, "The Early universe," Front. Phys. **69**, 1 (1990).

[43] Andrew R. Liddle and David. H. Lyth, Cosmological Inflation and Large-Scale Structure, Cambridge University Press, 2000.

[44] J. D. Barrow and S. Hervik, "Anisotropically inflating universes," Phys. Rev. D **73**, 023007 (2006) [gr-qc/0511127].

[45] J. D. Barrow, D. J. Shaw and C. G. Tsagas, "Cosmology in three dimensions: Steps towards the general solution," Class. Quant. Grav. **23** (2006) 5291 [gr-qc/0606025].

[46] Wiltshire, David L. (2007). "Exact Solution to the Averaging Problem in Cosmology". Phys. Rev. Lett. 99 (25): 251101. arXiv:0709.0732. doi:10.1103/PhysRevLett.99.251101

[47] Mustapha Ishak; James Richardson; David Garred; Delilah Whittington; Anthony Nwankwo; Roberto Sussman (2007). "Dark Energy or Apparent Acceleration Due to a Relativistic Cosmological Model More Complex than FLRW?". Phys. Rev. D 78 (12). arXiv:0708.2943

[48] Teppo Mattsson (2007). "Dark energy as a mirage". Gen. Rel. Grav. 42 (3): 567599. arXiv:0711.4264

[49] Cruz, Martnez-Gonzlez, Vielva & Cayn (2005), "Detection of a non-Gaussian Spot in WMAP", MNRAS 356 29-40

[50] Inoue & Silk, 2006, "Local Voids as the Origin of Large-Angle Cosmic Microwave Background Anomalies I", ApJ 648 23-30

[51] T. Padmanabhan, Structure formation in the universe, Cambridge University Press 1993.

[52] S. Dodelson, Modern Cosmology, Academic Press 2003.

[53] A. Challinor, Large Scale Structure formation Notes, Cambridge, 2008.

[54] H. J. Mo, F. V. D. Bosch and S. White, Galaxy Formation and Evolution, Cambridge University Press, 2010.

[55] U. -L. Pen and P. Zhang, "Observational Consequences of Dark Energy Decay," arXiv:1202.0107 [astro-ph.CO].

[56] Vishniac, E. T. 1987, ApJ, 322, 597

[57] L. D. Shaw, D. H. Rudd and D. Nagai, "Deconstructing the kinetic SZ Power Spectrum," Astrophys. J. **756** (2012) 15 [arXiv:1109.0553 [astro-ph.CO]].

[58] Gunn, J.E.; Peterson, B.A. (1965). "On the Density of Neutral Hydrogen in Intergalactic Space". Astrophysical Journal 142: 16331641.

[59] Becker, R. H.; et al. (2001). "Evidence For Reionization at z 6: Detection of a Gunn-Peterson Trough In A z=6.28 Quasar". Astronomical Journal 122 (6): 28502857. arXiv:astro-ph/0108097

[60] W. Hu, "Reionization revisited: secondary cmb anisotropies and polarization," Astrophys. J. **529**, 12 (2000) [astro-ph/9907103].

[61] Scoccimarro, R., Sheth, R. K., Hui, L., & Jain, B. 2001, ApJ, 546, 20.

[62] D. H. Rudd, A. R. Zentner and A. V. Kravtsov, "Effects of Baryons and Dissipation on the Matter Power Spectrum," Astrophys. J. **672**, 19 (2008) [astro-ph/0703741 [ASTRO-PH]].

[63] `https://pole.uchicago.edu/blog/`

[64] `http://www.princeton.edu/act/`

[65] Gnedin, N. Y. & Hui, L. 1998, MNRAS, 296, 44

[66] A. Hojjati, L. Pogosian and G. -B. Zhao, JCAP **1108**, 005 (2011) [arXiv:1106.4543 [astro-ph.CO]].

[67] C. L. Reichardt et. al., A Measurement of Secondary Cosmic Microwave Background Anisotropies with Two Years of South Pole Telescope Observations, The Astrophysical Journal, 755:70 (23pp), 2012 August 10